Klinik und Poliklinik für
Mund-Kiefer-Gesichtschirurgie
der Technischen Universität München
Klinikum rechts der Isar

(Direktor: Univ.-Prof. Dr. Dr. Dr. h.c. (UMF Temeschburg) H.-H. Horch)

3D Interactive Segmentation – First Applications for Computer-Aided Craniofacial Surgical Planning

Lutz Ritter

Vollständiger Abdruck der von der Fakultät für Medizin der Technischen
Universität München zur Erlangung des akademischen Grades eines

Doktors der Medizin

genehmigten Dissertation.

Vorsitzender: Univ.-Prof. D. Neumeier
Prüfer der Dissertation: 1. Prof. Dr. Dr. H.-F. Zeilhofer, Universität Basel / Schweiz
                          2. Univ.-Prof. Dr. Dr. Dr. h.c. (UMF Temeschburg)
                             H-H. Horch

1 Summary

An original and interactive approach to efficiently and accurately construct patient specific virtual 3-D models of the skull is presented. Computer-aided craniofacial surgery has many successful applications for patient individual 3-D models, e.g. virtual surgical planning of bone realignments, simulation of minimally-invasive distraction osteogenesis or generation of rapid prototyping models. However, generating the essential 3-D model for these applications can be a cumbersome and time-consuming task. In many cases this task can be divided into the following steps: image filtering, segmentation and surface reconstruction. While it is useful to consider each step of this pipeline separately for developing new algorithms, from a practical point of view these steps can be seen as a conglomerate yielding a 3D model as the final product.

Since each step has great influence on the following ones, the proposed interactive approach is embedded into a dedicated pipeline for the reconstruction of 3-D models of the skull. This pipeline consists of a statistical algorithm reducing metal artifacts, a filtering algorithm based on Markov random fields, a 3-D interactive segmentation using region-growing and thresholding algorithms followed by a dedicated implementation of the Marching Cube surface generation algorithm. The crucial point is a real-time segmentation approach providing the user with an instant volume view of the result. This approach avoids the time-consuming surface generation step when checking for segmentation errors in volume. All processing steps are represented as modules embedded in the software framework Julius, handling essential steps like data management and visualization. The pipeline was tested with 7 different cases for craniofacial surgical treatment with indications ranging from corrective bimaxillary repositioning osteotomies to complex reconstructions after tumor resection. It was shown that efficiency could be improved while quality of the segmentations was stable compared to manual segmentation.

2 Introduction

Most surgical interventions today are planned on the basis of various available radiological imaging techniques. X-ray pictures, interactive Ultrasound (US), high-resolution Computer Tomography (CT), Magnetic Resonance Imaging (MRI), as well as highly sensitive nuclear medicinal imaging methods as Positron Emission Tomography (PET) provide the surgeon with synergistic information of the patient's anatomy and pathology. In the case of tomographic scans they are usually visualized as grayscale images showing a two-dimensional (2D) cross-sectional slice of the patient's three-dimensional (3D) anatomy. Printed as a series of slices on radiological film they are analyzed. A surgeon has to mentally translate from the 2D grayscale slices back to the 3D patient anatomy and take this knowledge into the operating room (OR). There, he has to map all this information to the actual operating situs and operate with high dexterity.

The field of computer-aided surgery aims at supporting the surgeon at various steps from the imaging towards the actual surgical procedure. From inspecting the images for diagnosis, over planning and finally performing highly complex surgical interventions computers have been employed for assistance:

- Computers can be used to enhance the visual appearance of the acquired images. Contrast can be adjusted, noise reduced, edges sharply displayed and areas of interest zoomed [Ehr97, Tay96].

- Digital networks within and between clinics as well as great storage capacities of modern computers offer the possibility to efficiently distribute, store and visualize radiological images [Kru01, Eng99].

- Information of different modalities can be fused into one single image. This process named registration enables the surgeon to intuitively assess all the diagnostic information of his patient at one glance [Kro01, Zei97].

- Optimal donor sites for autologous bone grafts for reconstructive purposes can be determined by using surface matching techniques based on CT scans [Kro00, Mai98, Zei94].

- 3D representations of tomographic scans can be reconstructed and visualized from arbitrary views by computers [Van83].

- Virtual as well as real stereolithographic 3D models can be generated patient-individually and used as models for exact surgical planning and prediction of surgical outcomes [Kee98, Zei98, Del94].
- Computer-driven, image-guided robots can be used to precisely and constantly drill, cut and saw [Has97].
- Virtual surgical training devices and 3D representation of normal anatomy are used to enhance medical education and training [Pfl01].
- Tomographic scans and 3D models can be matched to the real operating scene and provide the surgeon with image guidance during surgery [Fer00, Has98, Mar98].

Craniofacial surgery was and still is one of the most active researching surgical subspecialties in the field of computer-aided surgery. The fact that a craniofacial surgeon has to consider the entirety of the human skull and the relationship between different bony facial structures quickly led to the idea of 3D renderings
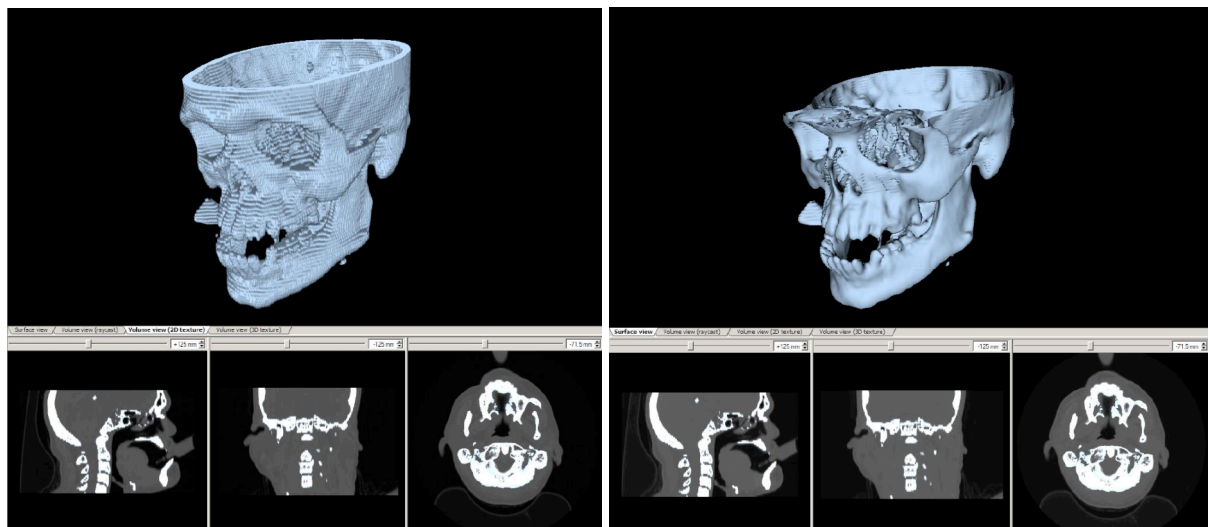
Figure 1: Two Screenshots of Julius: On the left the 3D interactive segmentation view shows a Volume Rendering of a cranial CT scan. On the right a 3D surface model of the same dataset, following a segmentation is shown.

of CT scans as approaching the anatomy slice-by-slice does not provide clear assessment of greater anatomical proportions [Van83].

Two kinds of 3D representations can be distinguished: 3D volume renderings and 3D surface models (See Figure 1). 3D volume renderings are easy to achieve and are very helpful in diagnosis of complex craniofacial deformities as the anatomy can be inspected quickly from all angles in 3D. However, 3D volume renderings

do not allow for virtual planning and building of stereolithographic models (see Figure 2).

3D surface models on the other hand can be used for more then just inspection: They can be virtually manipulated by the user (i.e. virtual osteotomies can be applied and dissected bone parts can be moved arbitrarily or stereolithographic models can be produced). Generating these 3D models however requires a number of subsequent computer processing steps [Eve00, Fro93, Kee98, Pel96, Sch99, Sad97, Zei98].

3 Rationale

Clinical applications of computer-aided surgery as interactive virtual surgical planning, building stereolithographic models, finding optimal donor sites for autologous transplants via surface matching and virtual surgical training programs require 3D surface models of the patients anatomy. The reason for that is computational speed on the one hand, since 3D surface models allow to be manipulated virtually in real-time, and the pure surface on the other hand to produce stereolithographic models.

A whole dedicated pipeline of subsequent computational steps has to be applied to the patient CT scan in order to build 3D surface models. After image acquisition the data needs to be digitally transferred to a computer workstation. Here filters may be applied to the data in order to enhance the quality of the scan or to remove acquisition artifacts. Then, segmentation, that is delineating the structures of interest in the radiological data, has to be performed. Finally, the segmented data has to be reconstructed to a 3D model yielding the basis for further applications such as virtual surgical planning (see Figure 2) [Tay96].
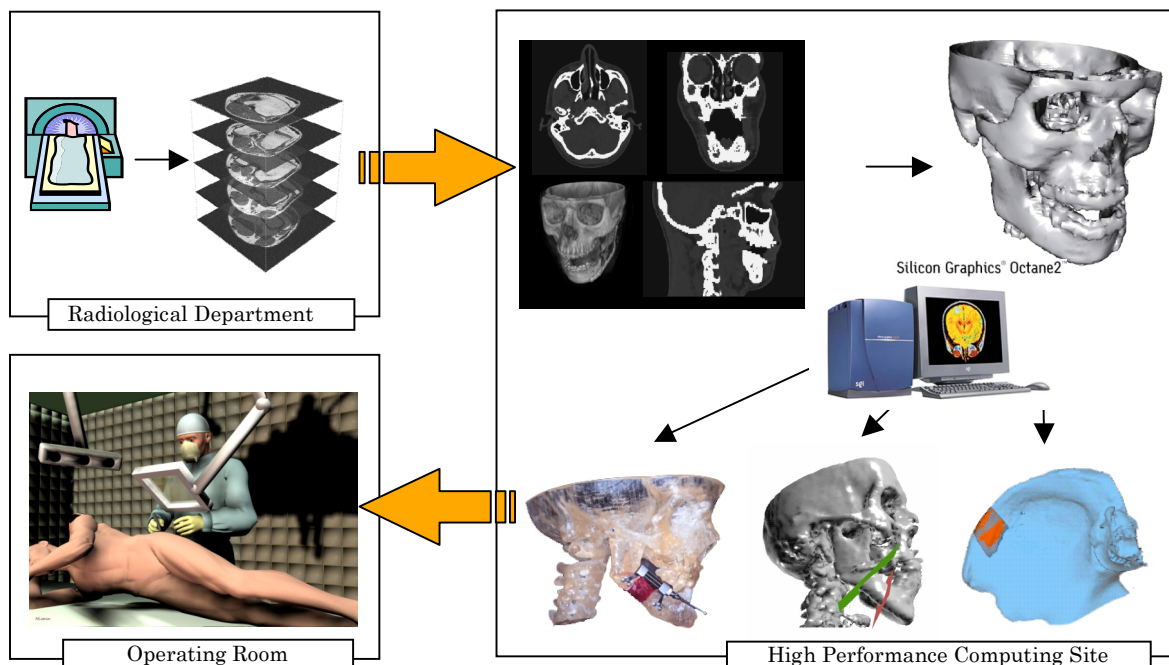
Figure 2: Common work steps in computer assisted surgical procedures based on tomographic images: After image acquisition in the radiological department these are transferred to a computer to be visualized, filtered and processed to a 3D model. Subsequent applications as for example RP models or virtual surgical simulations are based on these 3D models. All these techniques can be finally applied to guide the surgeon in the operating room.

Segmentation, as a central step, is influenced by prior steps as image acquisition, image management, image enhancement algorithms and how the images are visualized. Due to the high complexity of segmentation but in contrary to its importance, segmentation remains a bottleneck in building 3D models from patient medical images. One the one hand delineating the human anatomy and pathology displayed on tomographic slices is highly complex. Imaging artifacts frequently lessen the diagnostic value and image resolution is not always sufficient to pick up delicate anatomical details. On the other hand, automatic software tools for segmentation that are currently available do not achieve sufficient accuracy for medical applications. Manually driven segmentation tools lack intuitive user interfaces to perform the task efficiently. Consequently, segmentation appears as a time consuming task hindering surgeons to apply computer-aided surgical planning routinely. One major constraint in current segmentation tools was found to be the 2D visualization of CT data sets and the segmentation process. The segmentation is superimposed on the original sliced data set [AMI, ANA, MIM, SLI]. This method is established although it has several drawbacks:

- The user needs to inspect every single slice in order to verify parameter tuning of the manually employed algorithm.
- Global segmentation algorithms when applied to the whole volume are particularly hard to control using a slice-by-slice approach.

Some segmentation errors are only encountered by inspection of the reconstructed 3D model. As a consequence, iterative generations of 3D surface models during the segmentation, each taking at least several minutes, dramatically decelerate the segmentation process.

The goal of this thesis was to identify and develop an efficient but reliable processing pipeline to construct 3D models for computer-aided craniofacial surgical planning. As outlined above, this pipeline consists mainly of the following tasks:

- Data Management
- Image Enhancement
- Segmentation
- Surface Reconstruction

First, available software packages were reviewed focusing on their capability to perform the aforementioned processing steps and their general handling. The knowledge and experience gathered helped to develop and evaluate, in cooperation with a computer scientific research group, software that would enable one to perform each of these steps using an intuitive and interactive user-interface. This would ideally yield a software wizard guiding the user from the CT scan to creating a 3D model in a time efficient and accurate manner while leaving the user visual control over the process.

Tracking this ambitious task, the development and evaluation of a new segmentation technique was focused. Together with a computer scientific group at the research center caesar the idea of bringing the intuitive 3D real-time rendering of CT scans into the segmentation process was followed yielding the concept of 3D interactive segmentation.

This approach promises to overcome some of the current limitations of the segmentation tools visualized in 2D. Selected algorithms and tools for prior data management, image filtering and subsequent surface reconstruction to complete the required processing pipeline supplemented the approach. This pipeline was integrated into the software framework Julius providing the essential software developer tools and a graphical user interface.
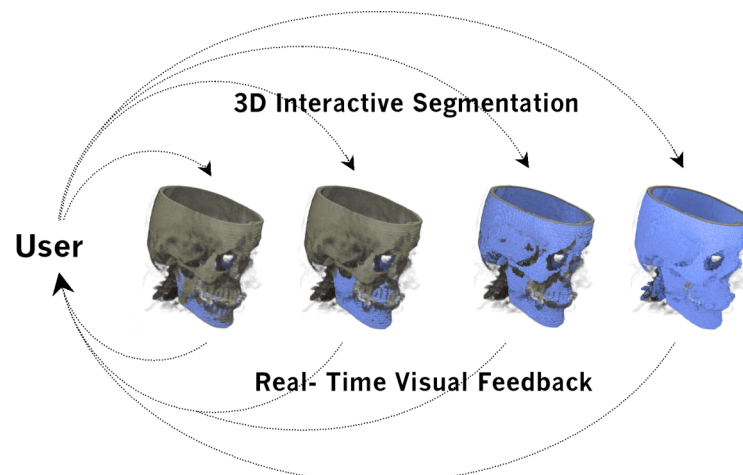

Figure 3: The Concept of 3D interactive segmentation implies that the user receives real-time visual feedback in 3D to his segmentation. Here the volume rendering of the initial data set is displayed in gray while with decreasing threshold the segmented pixels are shown in blue.

4 Related Work

Several software packages in the field of computer-aided surgery were reviewed. Some are more related to processing pipeline presented here in a way that they are capable of performing all steps necessary for producing 3D models. These software packages are 3D Slicer [SLI], Amira [AMI], Analyze [ANA] and Mimics [MIM] and are closely related to the presented software package Julius.

Other very helpful software like ImageJ [IMJ] or Xmedcon [XME] were also reviewed but have a slightly different focus than the work presented here and are therefore not described in detail. As a focus of this thesis remains on the integration of the newly developed 3D interactive segmentation some related work specifically for this topic is also presented.

Software packages for digital image processing can be roughly classified following their functionality:

- 2D visualization, measurement and management
- Application driven (included in scanners or any other hardware)
- Multipurpose stand-alone

Good examples for the first class are Osiris [OSI], Xmedcon [XME] or Image J [IMJ]. A group at the University of Geneva Switzerland developed Osiris, Xmedcon is an open-source project on source forge and ImageJ was developed by the United States National Institute of Health.

All tools are available free of charge for different platforms (i.e. computer operating systems). They are useful for visualizing tomographic scans or planar radiographs in 2D on any computer. They support a variety of image formats like Dicom, Raw and even the Analyze format (see Chapter Image Formats). Gray value representation can be arbitrary changed; reslicing of volume data sets is possible if other dimensions are needed. Surface and volume measurement tools are provided along with simple segmentation tools as threshold and manual segmentation for volume and planar measurements. Filtering algorithms as mean or Gaussian for example are available on Image J (see Chapter Image Enhancement). None of these software tools offers functionality for operating a Dicom server nor 3D reconstruction algorithms for 3D model generation are

available. However, these three rather similar software tools work very reliable and are highly valuable for the analysis and 2D image processing.

For the second group specific software that is inherent to a certain scanner or other hardware can be listed. Siemens's Syngo is an example for such software that exceeds simple 2D visualization and patient management by far. However, in order to access such software one usually has to access the accompanying scanner, which made it impossible to the author to further review this software. Julius belongs to the third group and is capable of importing various image formats, apply sophisticated segmentation algorithms and reconstruct 3D models from segmented volumes. Software with similar or even more functionality was reviewed in more detail.

4.1 3D Slicer

The 3D Slicer was developed at the Surgical Planning Lab., Boston, U.S.A. [SLI]. It is available to the public for free download and offers functionality to visualize and segment medical images. It works on PC's as well as Sun Solaris Workstations. The 3D Slicer is well documented and email support as well as a newsgroup support is available.

3D Slicer only reads Raw format images. When converting Dicom files into Raw some information may be lost and the header for these images has to be edited manually. To overcome this problem 3D Slicer offers to save volumes as MRML (Medical Reality Markup Language) files that include all necessary information to load a data set. The MRML file format is based on XML (Extensible Markup Language)[XML]. However, basic knowledge of path and file structures on a UNIX operating system is necessary in order to use it on a powerful UNIX workstation.

Basic filtering algorithms are available as median or Gaussian filtering. 3D Slicer visualizes medical volume data sets as perpendicular 2D slices; volume rendering is not supported. After segmentation it visualizes 3D surface models sufficiently fast with several options. The models can be arbitrarily colored and shaded, offering many possible ways of visualization. Very useful is the clip plane option where the 3D model is visualized with arbitrary arranged 2D slices cutting the 3D surface model (see Figure 5).

Several basic segmentation tools are available. The most important are threshold, manual segmentation, morphological operations (i.e. eroding and dilating binary segmented datasets) as well as island removal (i.e. removing remaining islands within the segmented volume of defined size).

Segmented structures are reliably reconstructed to 3D models by the marching
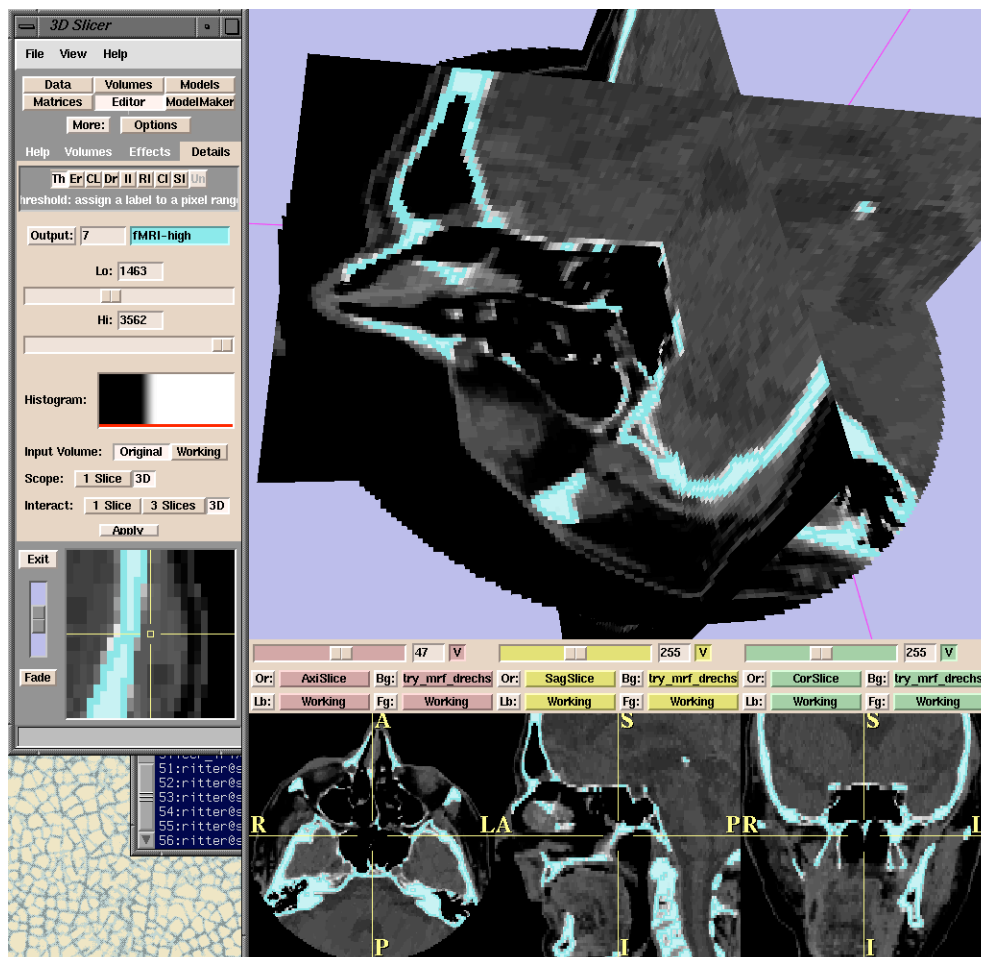
Figure 4: Perpendicular views on the 2D threshold segmentation with the 3D Slicer. On the left part of the picture the user can define the upper and lower threshold with two sliders. The pixels according to the threshold are colored in blue and superimposed on the original gray value data set as can be seen on the right part of the picture.

cubes surface reconstruction algorithm [Lor87]. The tools are concisely arranged making the 3D Slicer a versatile tool for basic segmentation that can be applied to a variety of clinical and research tasks: The 3D Slicer is provided with algorithms for semi-automatic registration (aligning data sets of various modalities e.g. CT and MRI datasets from one patient) and quantitative analysis (measuring distances, angles, surface areas, and volumes) of various medical scans. A wider range of applications provided by the 3D Slicer for intra-operative navigation and surgical planning can be found in literature [Ger99].

The 3D Slicer is a tool that is actively developed, therefore new versions may be available that exceed the functionality described in this thesis

Figure 5: 3D Slicer screenshot showing the clipplane option. Here 3D model and original MRI data set are visualized in the same view, whereas the 3D model is cut at the height of the perpendicular slices views at the bottom.

4.2 Analyze

Analyze is a software toolbox for computer-based techniques for the display and analysis of multidimensional biomedical images. The Biome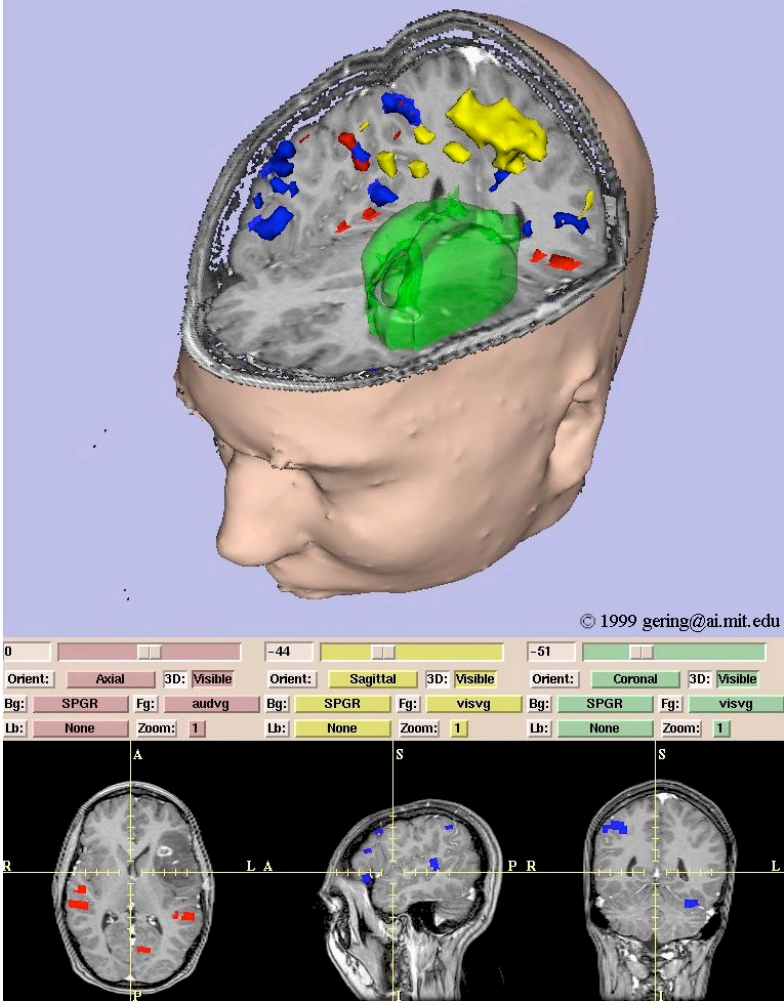dical Imaging Resource, Mayo Foundation, U.S.A., has been developing it since the early 1970's. It is distributed through Analyze Direct and depending on the license about 10000 Euro. Analyze works on several Platforms as PC or UNIX workstations and its implementation is based on Tcl/Tk [Tcl]. Analyze comes with a sophisticated documentation that leads the user trough tutorials unveiling the various functions of the software.

Analyze can handle over 30 different data formats as Raw or Dicom. It robustly sorts slices of a volume dataset automatically and converts these into its own Analyze data format. This format has the advantage to combine the slices of a volume into one file making data management more comfortable. However, many other software packages cannot read the Analyze format, making it somewhat incompatible for further processing.
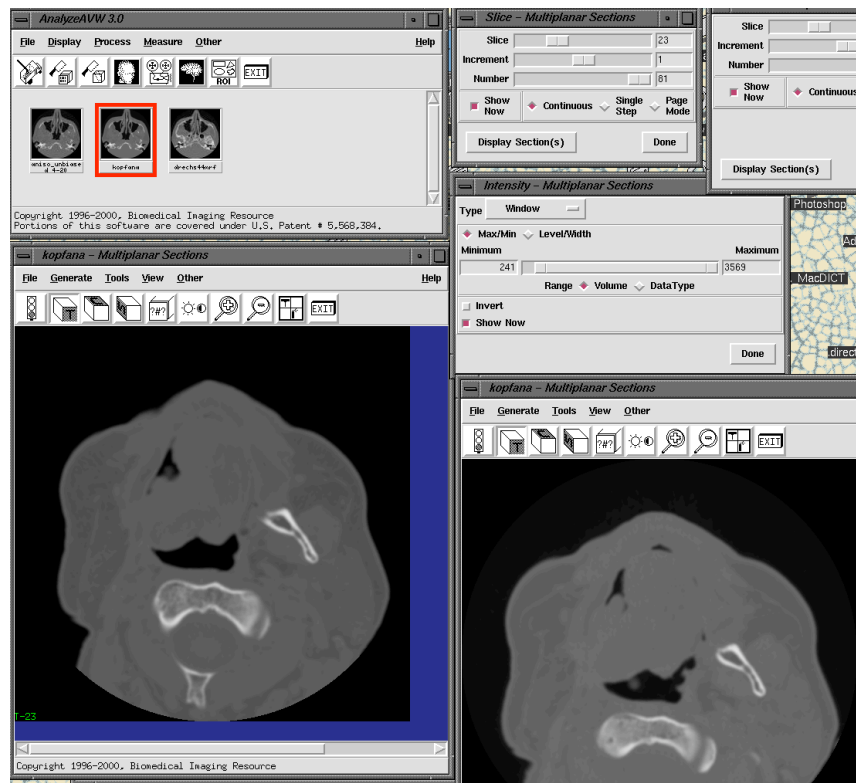

Figure 5: Analyze displaying several slices of a cranial CT scan. On the top left the data management window displays the available data sets. On the top right there are the tuning bars for orientation within the volume and viewing options as center and width. Note that due to the Tcl/Tk architecture for each module a new window is opened which might sometimes confuse.

The user can choose from a comprehensive selection of different filtering and enhancement algorithms that can be tuned to specific problems (see Chapter Image Enhancement). However, the user needs a minimum knowledge of filtering techniques in order to achieve meaningful results. Basic filters as median or low pass are available as well as more sophisticated as anisotropic diffusion filtering or even custom designed algorithms. Each filter comes with several parameters to tune for each operation. Giving so many filtering options the advanced user has virtually no limits. However, little documentation is available on which filter is applicable for any particular application leaving non-professionals following a trial and error concept.

Analyze offers 2D slice visualization and initial volume rendering. After segmentation, 3D models can be reconstructed from a selection of several algorithms. While there is a wide selection of surface reconstruction algorithms the inexperienced user needs some time to take full advantage of it due to tricky parameter tuning.
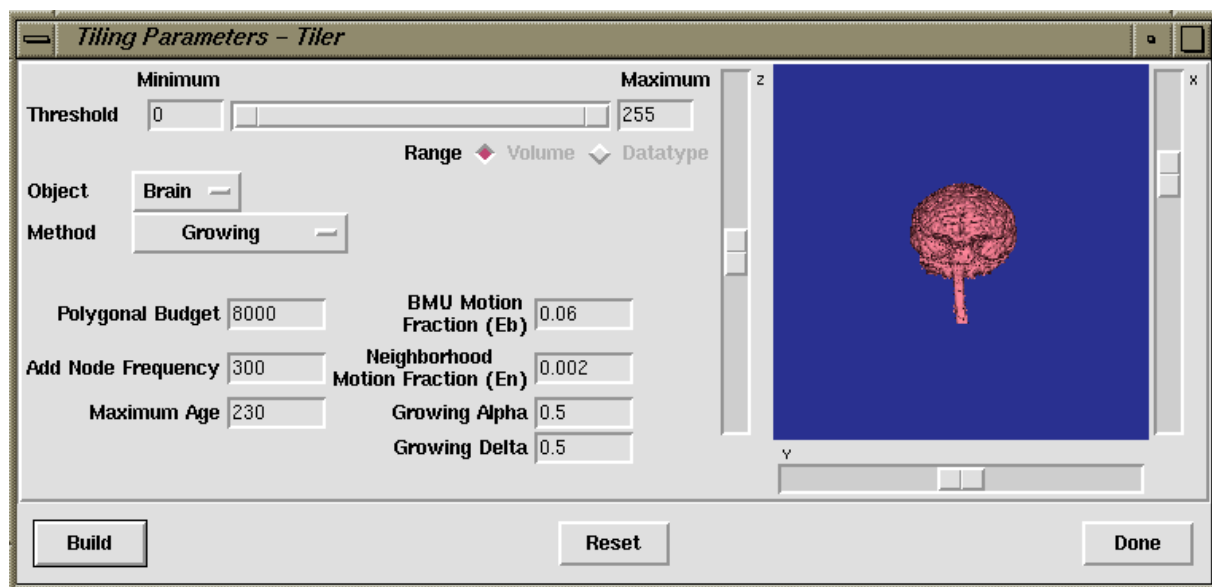
Figure 7: Tiler user interface of Analyze for surface reconstruction. Several parameters can be tuned by moving a slider or typing in numbers.

The visualization tools of Analyze include surface, volume and slice rendering. Moreover, movies of arbitrary scenery can be generated.

Analyze provides powerful segmentation tools. The suite includes sophisticated manual segmentation tools that by far exceed just drawing with different sized paintbrushes. Splines, various polygons and filling tools are

present that enhance the manual segmentation process. Other segmentation algorithms as threshold, morphological operations and automatic edge detection are provided as well. Especially interesting is the step editor that was implemented to line up different segmentation algorithms in order to customize them for one specific application. This approach can be very useful to routinely segment similar data sets. Analyze also provides registration algorithms for inter modality fusion as well as surface matching.

Analyze is probably one of the most complete and sophisticated software packages for medical image post-processing. Using the step editor in Analyze it is even possible to customize a certain arrangement of vast amount of given algorithms to a pipeline that can be reused. Obviously, covering such a broach spectrum Analyze does not provide customized solutions for particular problems.

4.3 Amira

The Amira software package was developed at the Konrad-Zuse-Institut in Berlin, Germany and is commercially available. It covers a wide range of applications and was not specifically developed for medical applications. As a commercial release, Amira is very stable and well-finished software that supports many different data formats and runs on windows as well as SGI operating systems. The Dicom standard as well as TIFF, JPEG, Raw data, PLY VRML and other can loaded into Amira. However, the Dicom loader does not always recognize complete datasets but identifies images belonging to one dataset separately (i.e. scout images are recognized separately). The open-file dialog does not provide all the information available from the Dicom dataset and therefore the user has to load and inspect all the data manually.

Amira is equipped with a very intuitive user interface that represents data, visualization and processing steps as boxes. These boxes can be connected arbitrarily in a graphical user interface via drag and drop making it very easy for the user to perform complex operations (see Figure 8). Options for each box are displayed below the "box field" and can be manipulated easily and fast.

Amira offers arbitrary slice views as well as volume and surface rendering techniques. The handling is adequately fast and intuitive.

Different filtering and segmentation algorithm are provided. For segmentation the standard view of Amira is changed for a dedicated segmentation editor that offers simple thresholding, manual segmentation as well as special region-growing algorithm that is controlled by a so called lasso. The user clicks on a region in the image that is homogenic for some gray value and by dragging the mouse one can manipulate the particular threshold. Thereby is quite easy to even segment rather complex structures. However, this method is available for 2D interaction only forcing the user to segment slice by slice.

The segmentation is organized by the well-known label technique. That is for each structure the user wants to segment a label can be created and individually modified. To create a meaningful model the user does need some practice and patience since it is not that easy to handle the labeling technique of Amira. All segmentation algorithms except the threshold are visualized in 2D as an overlay on the original dataset. The threshold segmentation can be visualized in 3D but the segmentation process does not show the original dataset in 3D. Thereby the user can inspect the resulting 3D model but cannot compared to the
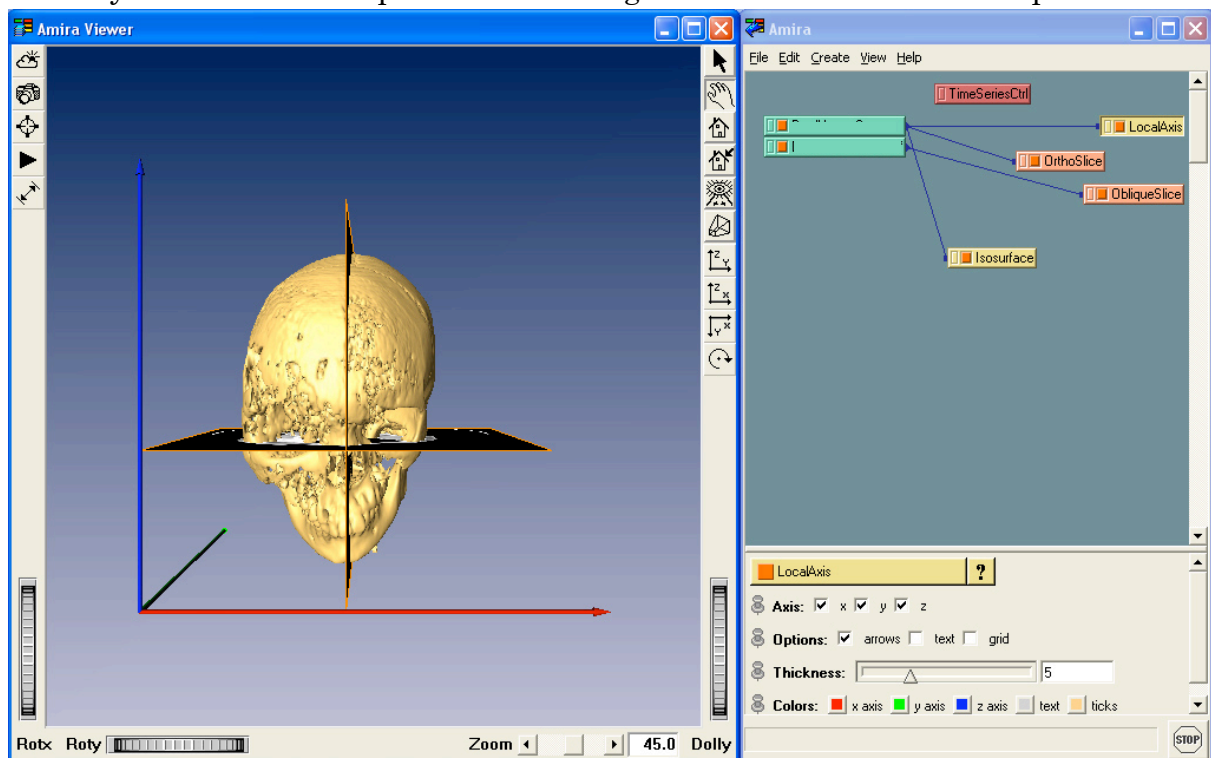
Figure 8: Amira standard view showing a segmented surface model on the left and the image processing and visualization interface on the right. Each box in this fields represents either data (on left) or processing steps (on the right). Below the box field option for the active box are displayed.

underlying original data in 3D, but has to reassure his segmentation on the particular 2D slices (see Figure 9).

Registration of datasets can be performed either manually or automatically with Amira, however this functionality was not reviewed in detail. Amira covers a wide range of applications and different siblings of Amira are available for more specific task (e.g. 3D molecular analysis). Quantitative analysis tools can be used to measure 2 and 3D distances and volumes.

Amira provides a programmers interface to facilitate the integration of new functionality to the Amira software. This functionality was not tested.

Amira does not provide an interface for intra-operative navigation. However, Amira has been successfully used to plan craniofacial surgery and to simulate postoperative outcomes of orthognatic surgery.
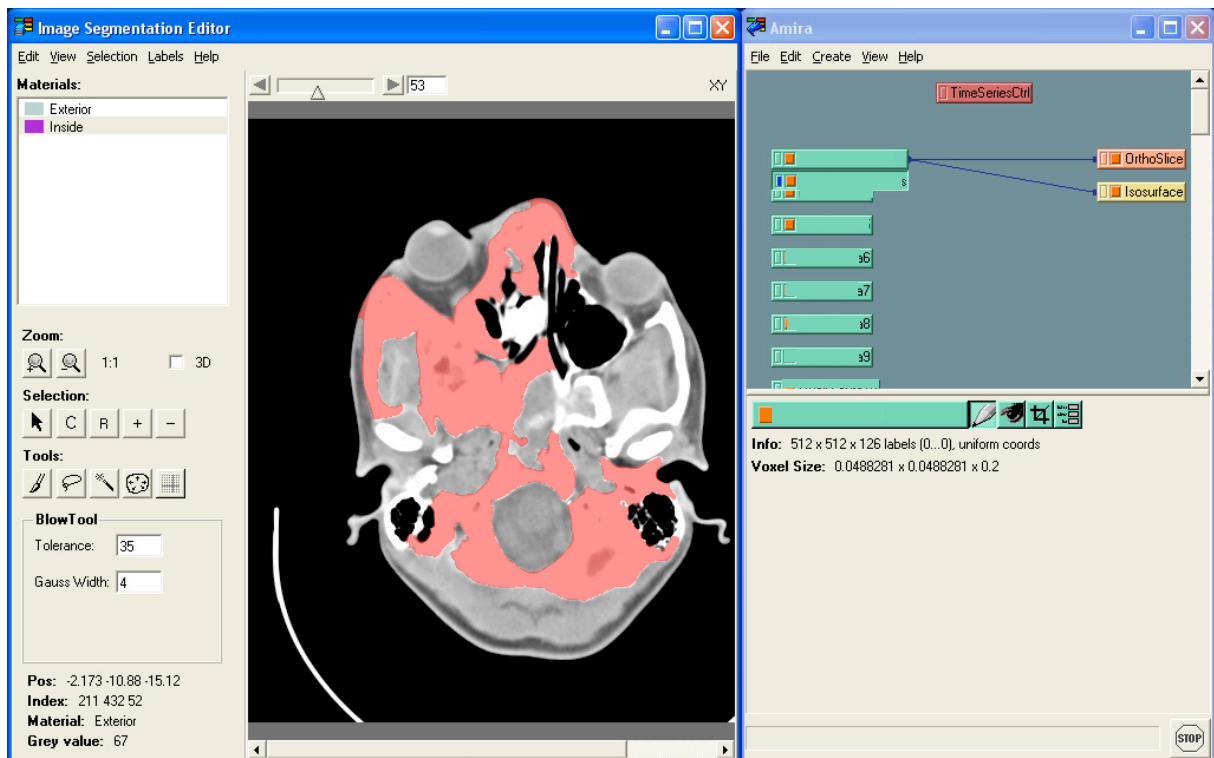
Figure 9: Amira segmentation editor showing a CT slice where bone is partially segmented using the lasso tool. On the left the different segmentation tools can be chosen and zoom and other visualization options can be tuned. In the middle the actual slice and its label are displayed. On the right the processing and data boxes are shown as well as their options.

4.4 Mimics

Mimics is a commercially available software package developed by Materialise, a Belgian company [MIM]. Mimics focuses on interfacing from medical scanners to rapid prototyping. Therefore Mimics cannot only generate STL(i.e. a standard file format for rapid prototyping) files but with additional software from Materialise most rapid prototyping machines can be managed. As a commercial product, Mimics is very stable and professionally designed. Mimics covers a wide range of different data formats using a special software for the conversion of data. This software can be acquired separately from Mimics, but Mimics inherently can read Dicom images. In addition to that Materialise offers a conversion service where images can be send to the company which then will convert them in the desired format.

CT and MRI images can be visualized and segmented. For segmentation several algorithms as thresholding, region growing, manual segmentation and

Figure 10: Mimics user interface with an axial view on the left and a coronal view on the right of a pelvic CT scan. A 3D reconstrution can be seen on the lower right corner with the different bony parts visible. On the right hand side viewing options can be tuned.

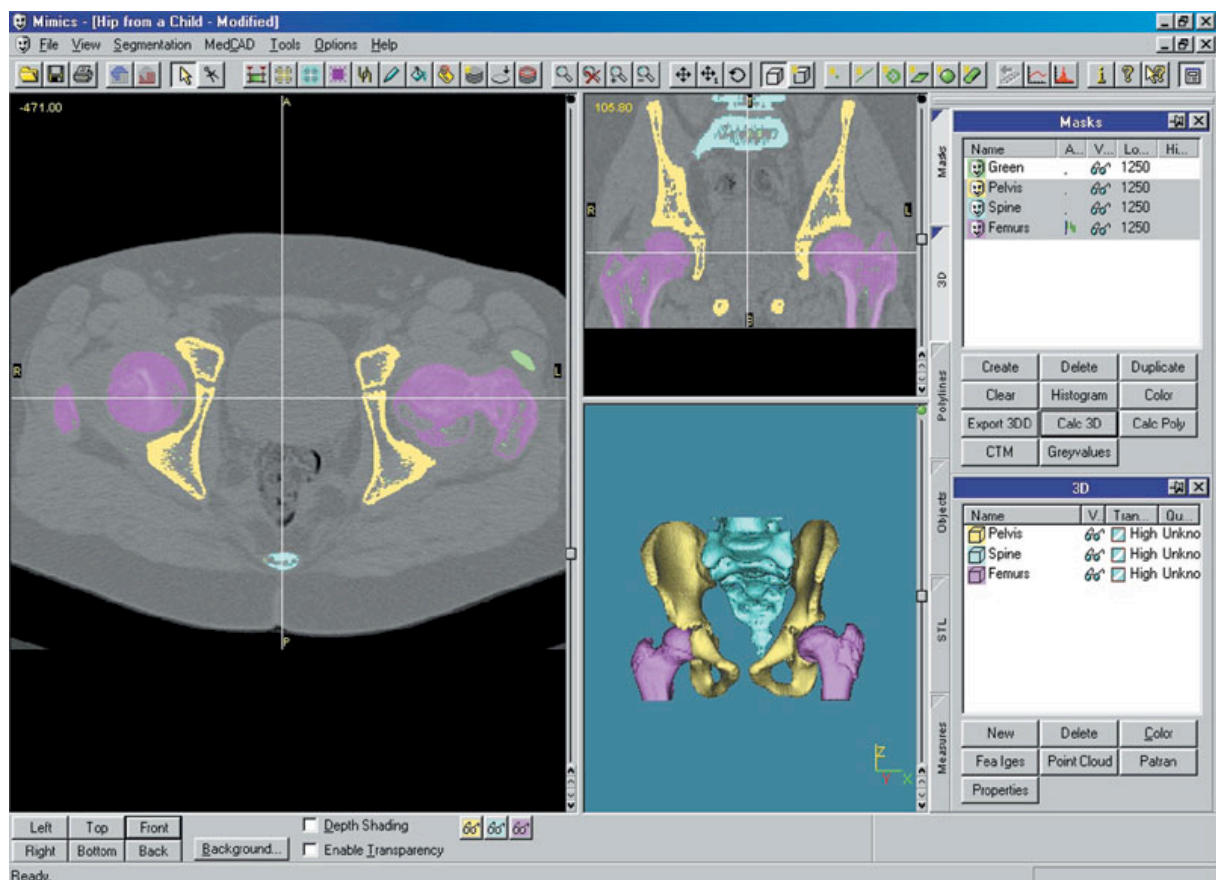morphological operations are available. All segmentation processes are visualized in 2D slices. Center and width of the original gray-values for the original dataset can be tuned as well as opacity and shading options for the visualization of 3D models are available. Point-to-point measurement tools for 2D slices and 3D models are available. Mimics offers also the possibility to generate finite element meshes to analyze and simulate for example strain-stress relations.

Mimics is a reliable tool for segmentation and visualization of CT images and is rather focused on producing 3D models for rapid prototyping. Along with other software available however, Mimics does also cover computer-aided planning of dental implants and intra-operative navigation using rapid-prototyping molds.

4.5 3D Interactive Segmentation

The idea of visualizing the segmentation process (i.e. the original and label data set during segmentation) interactively in 3D has been investigated before using different computer hardware and algorithms for segmentation and visualization.

Höhne et al. applied threshold segmentation as well as morphological operations (i.e. erosion and dilation of a binary volume) and visualized those in 3D, achieving an update rate of at least 5 sec per image on an IBM 3090/600 mainframe computer with an IBM 6090 graphics system attached [Hoe92]. By the time this pioneering work was able to provide the first generic 3D interactive segmentation tool in a research environment. However, availability of such computer hardware was and is still limited, and real interactivity could not be achieved yet which requires approximately 25 frames per second.

Saiviroonporn et al. were able to render segmentations of a 256x256x256 volume confined to a volume-of-interest below a second using a Connection Machine CM-200 with over 16000 CPUs [Sai98]. Connected component analysis as well as morphological operators were used for segmentation. Again, these were encouraging results, but very powerful and expensive hardware had to be used and data sets had to be confined to a volume of interest.

5 Material and Methods

In this chapter material and methods as scanner technique, patient data, computer hard- and software are described along with their implications for 3D model reconstruction.

The software to reconstruct 3D surface models for computer-aided surgical planning from patients CT scans is required to fulfill several processing steps as data management, image enhancement, segmentation and 3D reconstruction. A general introduction and criteria for successful performance for each of the processing steps is provided. These criteria were used to evaluate several methods for each processing step as well as the available software packages in total. To evaluate the newly developed 3D interactive segmentation as the most important processing step, seven models from original patient CT scans were created using 2D and 3D visualized threshold segmentation. The resulting models were compared in regards of construction time and accuracy.

5.1 Computer Tomography

In 1967 G. Hounsfield et al. developed the CT. Hounsfield linked X-ray sensors to a computer for assembling images from transmission data [Hou73]. Today CT images have a wide range of indications in medicine ranging from diagnosing neurological diseases to CT guided biopsies. Tomographic images are the essential basis for most applications in image driven computer-aided surgery.

The chapters about CT shortly introduce the basic techniques, scanner and protocols as well as parameters concerning the image quality. Special attention is drawn towards artifacts as features, which appear in the image but are not present in the imaged object. Additionally implications from the scanning process on 3D reconstructions are investigated.

In craniofacial surgery CT images are used as a valuable diagnostic tool to visualize bone and soft tissue anatomy and pathology. This visual information

forms the basis for planning complex resections and reconstructions involving bone.

5.1.1 Technique

In principle, a CT scanner consists of an X-ray source opposed by a detector measuring the X-ray attenuation from passing through the imaged object of interest placed on the gantry. This measurement is repeated from many different angles circling in one plane around the object. These X-ray shadows are directly related to the Fourier transform [Gol95] of the plane, and can be processed to reconstruct the cross-sectional slice of defined thickness [Doe00]. The distance between slices is defined as spacing. Each slice is represented as a matrix usually comprising 256 x 256 or 512 x 512 single points or picture elements (pixels). Each point represents the relative attenuation of a specific geometrical position in the object coded as a gray value on the picture. The higher the density of a position the higher the attenuation of X- rays, the brighter it is displayed in the reconstructed image.
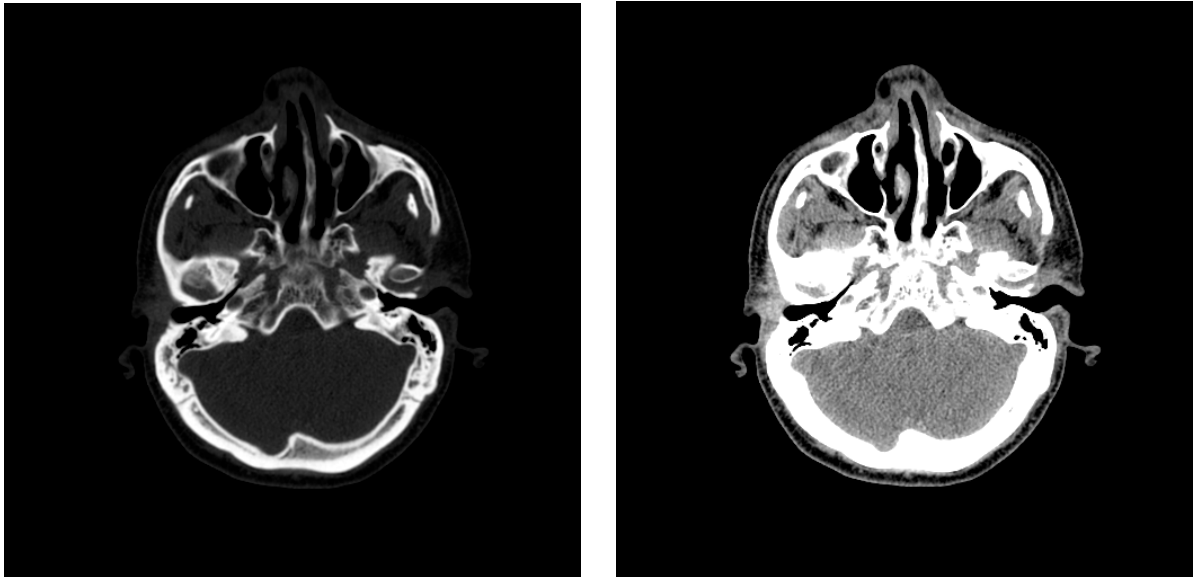
Figure 11: Two different visualizations with altered gray value distributions of the same slice of a cranial CT scan. On the left, bone structures are highlighted. On the right softtissue is highlighted.

Originally these gray values were represented numerical as Hounsfield Units (HU) ranging from –1000 HU for air, 0 HU for water to a total extent of around 3000 HU for very dense structures. However, the human eye can only percept up

to 20 different gray values limiting the visual representation. Hence, the displayed values have to be restricted to a defined window and center of the gray value representation [Csi99]. Different representations can be chosen to emphasize certain parts of the contained information (see Figure 11).

Subsequent scanning of slices finally yields volumetric information that can be thought of a stack of slices of defined size and spacing

5.1.2 Scanners and Protocols

By the assembly of X-ray source and detector four generations of CT scanners can be distinguished. Spiral CT scans are executed by simultaneous patient translation, gantry rotation and data acquisition. More configurations of CT scanners are known or in development, i.e. electron- beam CT scanner [Boy83], but should not be further discussed here.

Scanning protocols define the parameters for slice thickness, slice spacing, algorithms for reconstruction, image matrix and X-ray tube issues for each
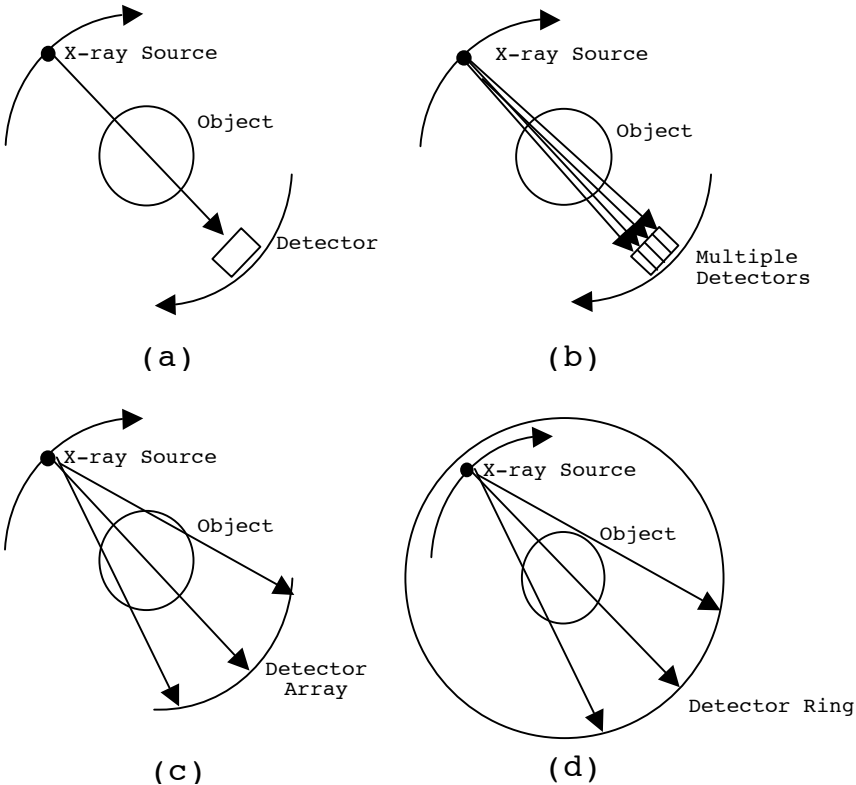

Figure 12: CT scanner architectures from first (a), second (b), third(c) and fourth generation (d).

individual scan. The whole scanning process can be adjusted to the clinical task in detail. However the parameters are confined to the technical specifications of the scanner used (e.g. the scanner is limited to a certain resolution).

5.1.3 Image Quality

Artifacts, image contrast and image resolution define the image quality of CT scans. Common artifacts include beam hardening artifacts, partial volume artifacts, motion artifacts and metal artifacts.

Beam hardening artifacts result from the physics of conventional X-ray sources for medical CT. These are rotating anode tubes, which have polychromatic spectrums. Hence, not all X-ray photons emitted from an X-ray tube have the same energy. As an X-ray beam traverses an object, the higher energy portion of the X-ray spectrum increases, since lower energy photons are attenuated more. If this nonlinear beam hardening effect is not compensated, a "cupping" in image gray-scale will be seen.

Partial volume averaging artifacts refer to a blurred appearance of discrete structures in a CT image. Since a reconstructed gray value is an average of attenuation within a voxel, edges inside of voxels cannot be displayed sharply.

Motion artifacts derive from movements of the examined body. These movements include voluntary as well as autonomic movements and usually result in blurring or CT number errors.

Metal artifacts usually originate from implanted materials like orthopedic prosthesis or dental fillings. The higher atomic number makes metal attenuate X-rays in the diagnostic energy range much more than soft tissues and bone. As a result, almost no photons penetrate the metal, and corresponding line integrals are lost. Dark and bright streaks around the metal part decline information contained in the image. These artifacts are also known as scattered radiation-induced artifacts that lead to cupping, streaks, and CT number errors.

Image resolution has three aspects: high-contrast resolution defines the ability to distinguish adjacent objects of high-contrast. Low-contrast resolution stands for differentiating an object from its background with similar attenuation values. Finally, temporal resolution characterizes the capability to resolve time-

varying structures. The parameters pixel size and spacing represent the spatial resolution in x, y and z direction of generated 3D scan volume, Therefore they are
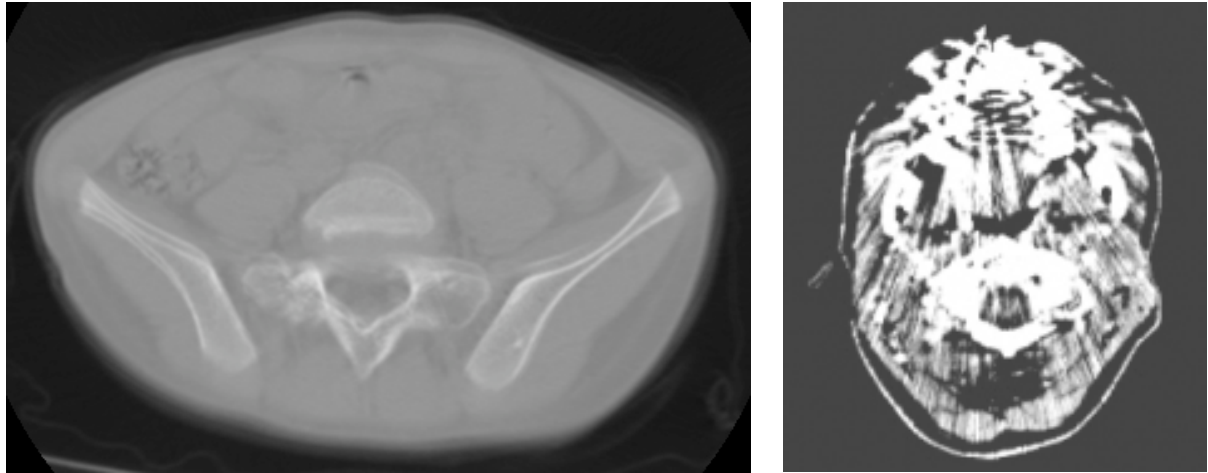

Figure 13: The left image shows motion artifacts from voluntary movement in axial slice of a CT scan of the pelvis. The right image shows metal artifacts from dental fillings in a axial slice of a cranial CT scan.

of vital importance for post-processing steps and 3D reconstruction. In general, with higher resolution in all of these parameters higher quality in the reconstructed 3D model can be achieved. However, radiological risk factors have to be considered, as higher radiation exposure for the patient might occur.

5.1.4 Implications of Image Acquisition on 3D Model Generation

Characteristics of CT scanning with the most significant influence on 3D model generation are related to the spatial resolution and artifacts of the scan. Especially the low resolution in the z-axis (i.e. spacing or the gap between slices) depicts as stair case artifacts on the 3D models [Obr01].

Additionally, with lower resolution, partial volume artifacts automatically increase, as pixel size increases. Adjusting scanning parameters to suit the desired purpose given adequate scanner hardware, however, can readily change these characteristics. Since the onset of multi-detector and helical CT scanners, sufficient spatial resolution for 3D model construction is technical achievable.

Artifacts caused by moving of the patient or metallic dental implants are less adjustable or require fairly invasive procedures to compensate for (i.e. sedation during the scan, removing teeth with dental fillings). On the other hand sophisticated filtering algorithms applied to the dataset can help to improve image

quality. Whenever correction or improvement is not possible, subsequent generated 3D models will appear significantly impaired.
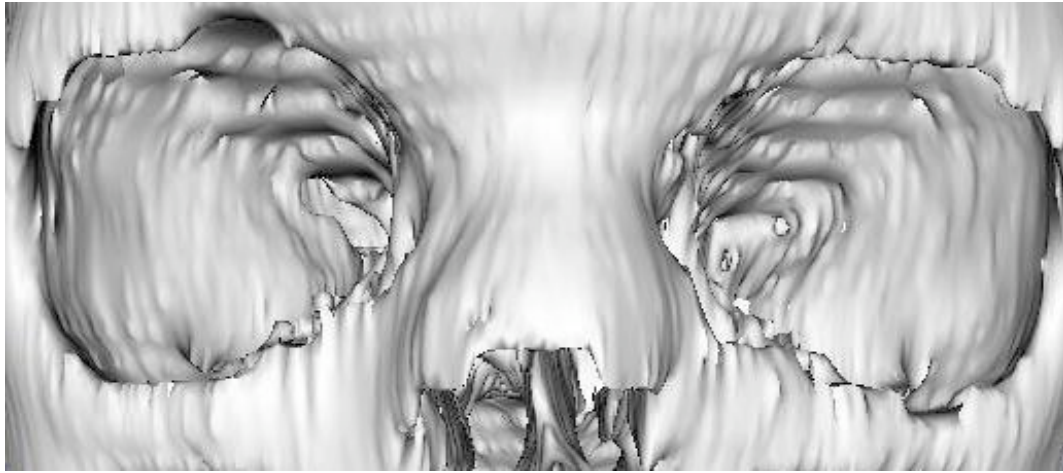
Figure 14: 3D model of the skull. Stair artifacts can be well appreciated on the superior wall of both orbits. This scan had 0.39 X 039 mm in x and y respectively and a 3mm spacing between slices.

5.2 Patient Data

Seven cranial CT scans from seven different patients with varying craniofacial pathologies were used to evaluate the introduced processing pipeline. All patients were treated at the clinic for cranio- and maxillofacial surgery of the technical University of Munich (Head: Univ. Prof. Dr. Dr. Dr. h.c. (TMF Temeschenburg) H.H. Horch).

All patients were scanned with a Phillips Tomoscan AV1 at the Technical University of Munich., department of radiology. The following table gives an overview of the used scan parameters and patients age. X and y spacing refer to the pixel size: on the image the size of one pixel on the x-axis represents x millimeter in that direction on the real patient; accordingly are the values for the y-axis on the image. The z-axis (i.e. spacing) numbers the millimeters between slices. The size of the data sets gives an impression of the immense data storage capacities that are needed for modern clinics today (i.e. these are cranial CT with an average number of slices of 84, for abdominal CT scans that number can triple!).

Pat. Number	X spacing (mm)	Y spacing (mm)	Z spacing (mm)	Pat age (years)	Slices	Size (Mbyte)	X-ray current
1	0.370821	0.370821	2	33	75	38.3	150
2	0.448942	0.448942	2	21	96	49.1	175
3	0.46833	0.46833	2	20	85	43.3	225
4	0.31222	0.31222	2	26	77	39.4	175
5	0.488	0.488	2	29	101	51.6	150
6	0.410084	0.410084	2	23	87	44.5	175
7	0.488	0.488	2	39	73	37.3	150
Average	0.42662814	0.42662814	2	27.29	84.86	43.36	171.49

Table 1: Scan parameters of the seven CT scans used for this study.

5.3 Computer Hardware

Several computers were used during the course of this investigation. The following table gives an overview of the most important specifications of the used hardware and information about which software was used on the particular computer.

COMPUTER	SIEMENS PC	SGI OCTANE	SGI ONYX 3200 IR3	SUN ULTRA 10
RAM	2GB	2GB	4GB	384 MB
CPU's x FREQUENCY	2x2GHz	2x400MHz	4x400MHz	1x400MHz
OS	WINDOWS 2000	IRIX / UNIX	IRIX / UNIX	SOLARIS / UNIX
GRAPHICS	ATI FireGL	V12	INFINITE REALITY 3	Elite 3D
SOFTWARE USED ON SYSTEM	JULIUS SLICER AMIRA MIMICS	PMOD	JULIUS ANALYZE	SLICER

Table 2: Computer Hardware and its specifications

All computers were linked within the caesar institution by a gigabit Ethernet network. A UNIX file server was used to shuffle and store the data.

The SGI Octane and Onyx stand out since they are built with shared memory architecture. Shared memory refers to the concept that the central

processing unit and the graphics unit use the same memory. That implies that the 4GB memory in case of the Onyx can be fully used for graphic applications exceeding the 256MB of 512MB of common graphic card.

5.4 Julius - A General Software Framework

The software-framework Julius served as a software development kit for the proposed processing pipeline in this thesis. New functionality developed in the context of this thesis was added to the previously existing functionality of the software framework Julius. This was achieved in tight collaboration between computer scientists and medical professionals. The idea of 3D interactive segmentation was developed in that collaboration followed by programming done by computer scientists and testing done by medical professionals. Julius is a general software framework for medical image processing offering a wide range of applications from surgical planning to intra-operative guidance. It provides an intuitive anatomy based user interface with sophisticated visualization algorithms. Julius was developed at the research center caesar, Bonn, Germany.

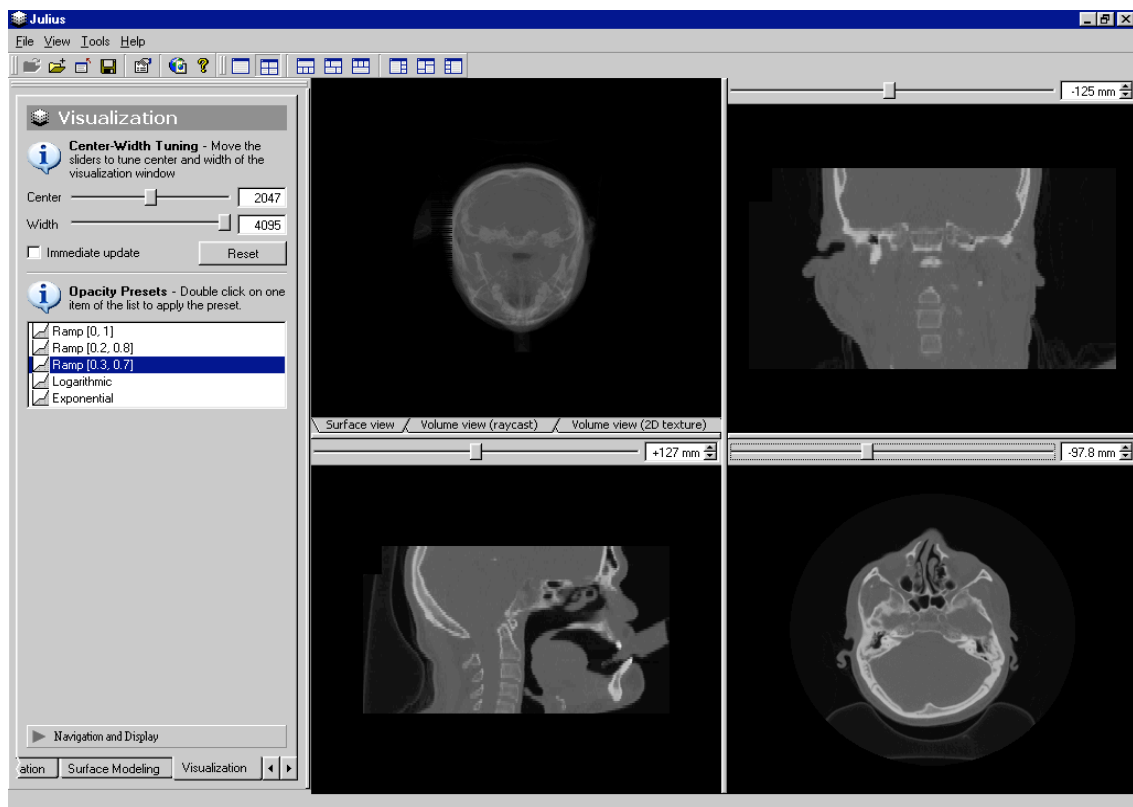Founded on QT and VTK [QT, VTK] it offers cross-platform compatibility

Figure 15: The Julius user interface in a standard view when a dataset is initially loaded.

for PCs, Apple Macintosh and various UNIX operating systems. As an open software framework Julius enables developers to easily integrate new algorithms and customize Julius to specific applications. Moreover developments presented here and more are available free on the Internet [JUL].

5.5 Data Management

This chapter gives a brief overview of ways and aspects of transferring medical images and image formats that are used in medical imaging. Criteria for an optimal data management are summarized in the end of this chapter.

5.5.1 Image Transfer

Radiological images of all modalities can be stored and transferred digitally today. The introduction of digital radiological images has brought many advantages and possibilities as for example digital image enhancement, fast and efficient information distribution within a medical facility or among cooperating clinical and research sites [Kru01, Eng99].

Computer-aided surgical planning critically depends on images in digital format and the electronic infrastructure. Picture archiving and communication system (PACS) are designed to handle data transfer and storage. However, very high demands as large data volumes to be stored, high image quality to be preserved and privacy to be kept makes handling medical image data somewhat complicated. This reflects a whole research and commercial field of its own offering professional solutions for data management.

In principal two different ways of transferring digital data can be distinguished: first, transfer via exchangeable storage media as compact discs (CD), magneto-optical discs (MOD), digital video discs (DVD), ZIP discs or transportable hard drives. Other exchangeable storage media as diskettes or tapes are somewhat cumbersome since diskettes do not provide sufficient storage space and tapes are very slow. Workstations as well as most personal computers are equipped with CD, DVD or Zip drives facilitating the use of such devices. On the one hand exchangeable storage devices are bulky if data has to be transferred

long distances or frequently, since the discs have to be mailed and data has to be copied on the discs manually. On the other hand, they are commonly available and safe to use, since third parties do not have access to them and data can be stored in a special code on the disc making it available only to designated people. Secondly, images can be transferred digitally using phone lines or digital network connections. The commonly known world wide web (WWW) makes transfer over great distances fairly easy and automatic to a certain degree. However privacy issues have to be concerned since any third party could possibly break into the system and have access to sensitive patient data. However, there are commercially available software package that incorporate safety measures generally sufficient for transferring patient data over the WWW [Eng99, PMO].
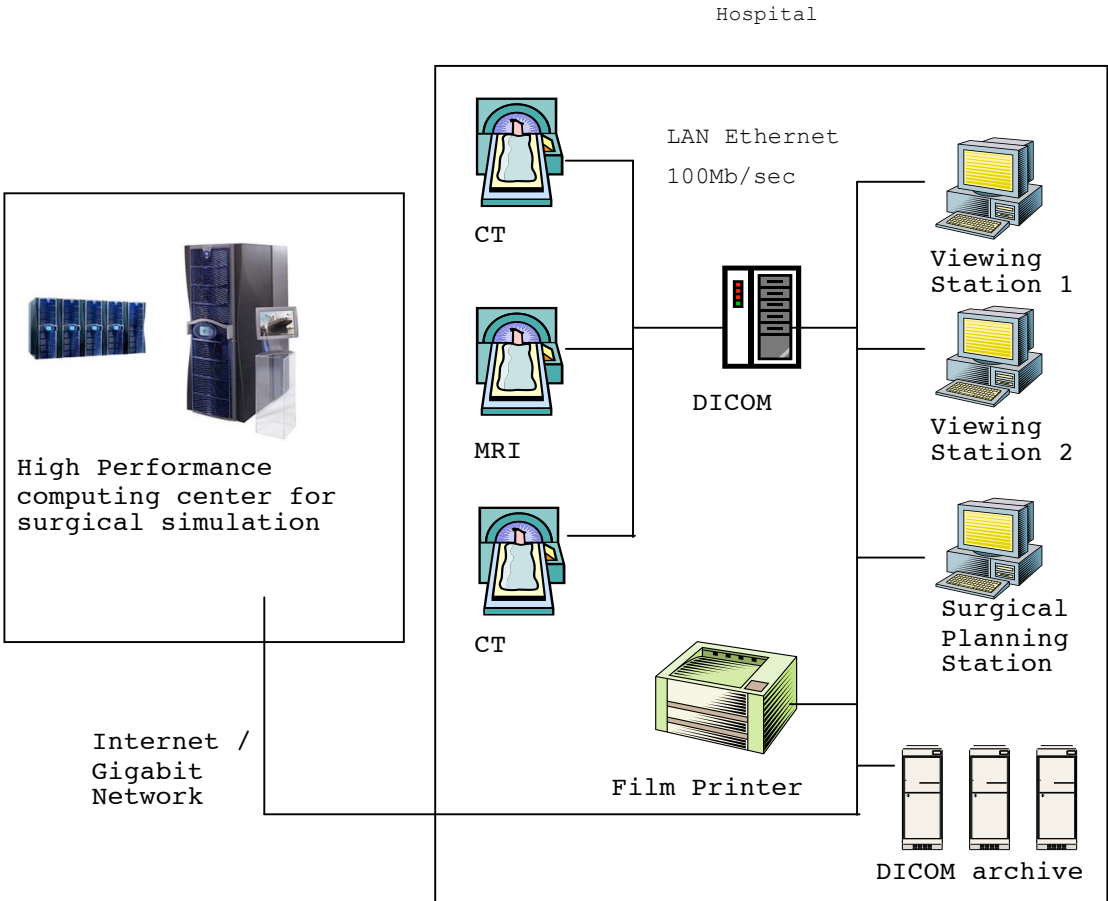

Figure 16: Possible setup of a picture archiving and communications system (PACS) linked to an external high performance computing site. Note that the actual user interaction takes place at the hospital parallel to other viewing stations.

5.5.2 Image Formats

Digital images are a matrix of points whereas each point is represented as a gray value. These gray values are stored digitally and in general 12 bits yielding 4096 different possible gray values for each point would be sufficient. This amount of gray values is required to adequately display radiological pictures. However, for performance reasons they are stored with 16 bits allocated (i.e. memory access in computers is much faster when memory pieces are in increments of 1 byte or 8 bit.). When considering the number of images produced in a hospital, only for tomographic medical scans, this requires large amounts of digital storage. For example, a dataset of a cranial CT scan as used in this thesis has a size of approximately 43 Mbytes in average (See Table 1). To efficiently store these images digitally, algorithms are used to compress the image. These can be divided in loss and lossless algorithms, which refers to the fact whether any information is lost during the compression, or not. Generally, lossless compression is used for medical images. The technical way in which the 16 bits per point for all points are arranged in the computer memory and whether or not the image is compressed, defines the image format. Commonly used in the area of computer aided surgical planning are Raw and Dicom. While the Raw image format is widely used outside the medical field, the Dicom format was specifically designed for medical applications. Unfortunately, many vendor specific sub-entities of the Dicom format exist, causing severe problems of compatibility for digital medical images even today [Ehr97].

The American College of Radiology (ACR) and the National Electrical Manufactures Association (NEMA) established the ACR-NEMA DICOM standard in 1993 [Bid92]. Dicom 3.0 represents the consequent development of the ACR-NEMA standards 1.0 and 2.0. The motivation was to establish a data format that all manufactures of radiological acquisition equipment would apply to, which is a requirement for efficient digital data management. Good improvements have been achieved in the last few years in this regard.

The Dicom standard describes how medical images can be digitally stored and transferred. Therefore to each image a header is added. This header contains

information about the used scan parameters, patient data, scan series, image resolution etc.

The Raw format on the other hand consists just like the Dicom format of header and image data, but the header reveals information about the image itself only. Resolution, spacing etc. are defined but usually no information about the patient or scan parameters is given. But often Raw images are used even without a header, and when using this data one has to enter the necessary information about the images to be loaded manually. Besides the fact that it is not according to the Dicom standard, it can be useful for privacy reasons.

5.5.3 Criteria For Efficient Data Management

The two most important aspects for efficient data management have been elucidated: compatible image formats as well as safe and fast data transmission. Software for the reconstruction of 3D models mainly has to deal with different image formats, since data transmission and Dicom server are capabilities that don not fall within the focus of such software. Therefore one has to consider whether or not the software can read the image format that is produced by a particular scanner (i.e. the scanner available for research purposes). However, it can be stated that the more image formats a software can read the better it is. Another aspect for data management is how segmented volumes and 3D models are administered within a software. From the standpoint of medical doctors it is desirable that a patient name based administration is provided, since this is the most intuitive fashion for medical doctors.

5.6 Image Enhancement

This chapter gives a short introduction of some general aspects of filtering medical images. Criteria particularly suited for filtering CT images in order to produce most realistic 3D models are brought forward. To choose the optimal image enhancement method for the proposed pipeline of processing steps, five different image enhancement methods were selected by the given criteria and visually compared. A short description of all tested filters is given. These are low pass filtering, median filtering, anisotropic diffusion filtering and Markov random fields filtering. Along with these established filtering methods a special filter to reduce metal artifacts was tested.

5.6.1 General Aspects

Algorithms for image enhancement reduce noise and artifacts or improve contrast within an image. In general, image enhancement algorithms transform pixel intensities of a given image to a new image following a mathematical function. The mathematical operations range from simple averaging of a pixel by its surrounding pixels to highly sophisticated adaptive anisotropic multidimensional filters. Basically there exist linear and non-linear filter operations. These can be further distinguished in rigid and adaptive filtering. As linear and non-linear describes the mathematical properties adaptive refers to changing the filter behavior according to the estimated properties of the image. These mathematical operations can be either applied in 2D or 3D space or the signal transformation (i.e. spatial and frequency domain) of a particular image (see Figure 17). Filtering in the frequency domain offers the possibility to apply filters not only on the reconstructed spatial 2D image but also on the underlying original frequency. Reasons for that are for example computational speed or assessing signals of the raw frequency data that are inaccessible after the reconstruction to an image. However, many filters can be applied to both domains.

Filters of the spatial domain usually work as a kernel. That can be imagined as an arbitrary set of points moving across an image (see Figure 17). Pixels within the kernel are respected for the given filter or transformation. Aside from this rather simplified classification, there exist numerous hybrids and modifications of the aforementioned methods. For explicit and rather technical reviews of filtering techniques the reader is referred to [Bal00, Ban00, Rus99].

It must be stressed at this point, that it is in general easier and more efficient to improve image quality at the stage of acquisition. However, radiological data is often impaired by noise and artifacts and therefore in need for image enhancement algorithms.
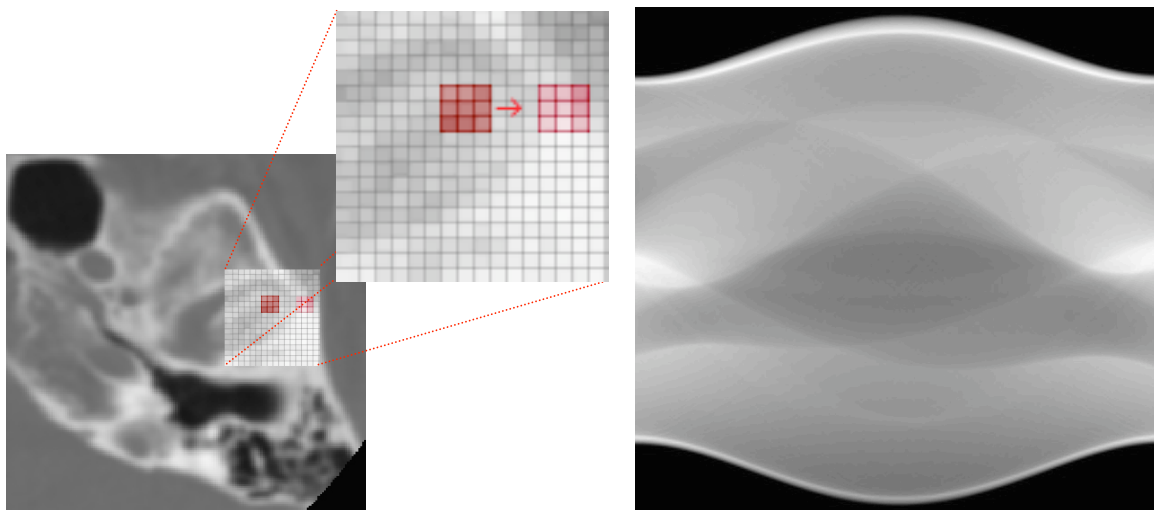
Figure 17: (A) describes the movement of a 3 x 3 kernel across the pixels of an image. (B) shows a typical sinogram. That is a graphical representation of the CT Raw scanner data.

5.6.2 Criteria for Image Enhancement of Medical CT Images

When choosing an algorithm for medical images enhancement several aspects have to be considered [Ban00, Kru01]:

- Data characteristics (noise, artifacts)
- Further purpose (e.g. enhanced human vision vs. automatic segmentation)
- Filter characteristics
- Available time frame
- Parameter complexity

For this study CT images were used and here noise is primarily determined by the dose setting of the X-ray tube, the slice thickness, the reconstruction algorithm, the characteristics of the CT scanner and the structures scanned in the field of view (see Table 1). These data-characteristics had to be taken for granted in this retrospective study since no influence could be taken on the scanning parameters. The datasets were chosen to have the best image resolution possible at that time and to be as homogenic as possible. Thereby sufficient detail for 3D reconstruction and comparability could be achieved. Metal artifacts from dental fillings in general often affect Cranial CT scans.

Threshold based segmentation algorithms as tested in this thesis are critically dependent on high image contrast. This contrast can be severely hampered by the partial volume effect.

The characteristics of each filter are described in detail in the following chapters. The available time frame is often rather short in a clinical setting, making this instance crucial for the practical value of a given filter method.

Related to the time criteria the handiness of a filtering method is very important. Some filters are very complex and require parameter tuning by an experienced person to achieve acceptable results. Eight to ten parameters represented by numbers are often encountered. If one wants to achieve standardized results when filtering images parameters have to be kept constant limiting the ability to adjust to special characteristics of a given dataset.

In conclusion it can be stated that a filter enhancing image contrast while diminishing artifacts that was also fast, easy to use and adaptive to image features was anticipated.

5.6.3 Low Pass Filtering

The low pass filtering is a commonly used linear filter. It dampens noise and averages or smoothes the image by replacing the pixel value with the average value of the specified neighborhood. The Kernel options are enabled to specify the neighborhood in size and shape. Image details that are small relative to the kernel are significantly suppressed while the degree of noise suppression increases with the kernel size. This filter can also be applied iteratively to finally

form a filter with approximately Gaussian weights – a smooth bell-shaped pattern that tapers gradually to zero. Kernel size, shape and iteration are parameters that have to be tuned.

For this thesis the low pass filtering functionality of Analyze [Ana] was used and images were filtered twice using a low-pass operation with a kernel size of 3 x 3 x 1 pixels. The filtered images were visually compared to the original image and to other images filtered with one of the other tested filters.

5.6.4 Median Filtering

The median filtering is based on statistical measurement that takes a given number of values and finds the value that splits the group of values into two equal halves. This value is called the median and represents a non-linear statistical measure. The number of pixels that is considered forms the size of the kernel. Together with the shape of the kernel these two parameters have to be determined by the user. The median filter is supposed to be less smoothing than the low pass filter due to the statistical measure taken. For this thesis the median filter functionality of Analyze and a kernel of 3 x 3 x 5 was used.

5.6.5 Markov Random Fields Filtering

The Markov random fields approach applies a low-pass filtering (smoothing) while still preserving edge information based on a statistical approach. This statistical theory is derived from Markov chains that extend temporal relationship to spatial neighborhoods. The associated theory assumes that the global description of one energy is equivalent to the minimization of local energies (i.e. adaptive filtering). This theory has been applied for image enhancement [Gem84] as well as for image segmentation [Hel97]. In image processing, the local energy is composed of two parts: a regularization function minimizing the noise of the observations on the data and a prior function adding locally spatial constraints as non linearity, non isotropy or 3D, on the final field. This algorithm is generally used as a regularization process, iterating over the

image until the stability or minimum energy is reached. The minimization of the noise, generally modeled as Gaussian additive, produce noise free images. The prior constraints increase the homogeneity and the contrast between anatomical areas. Thanks to the statistical theory, noise estimation allows this algorithm to be automatic, without any user parameter tuning.

5.6.6 Anisotropic Diffusion Filtering

Anisotropic diffusion filtering is a nonlinear operation that adapts to local image features. Noise is smoothed locally, 'within' regions defined by object boundaries whereas little or no smoothing occurs between image objects. Instead it enhances local edges since discontinuities, such as boundaries, are amplified. The idea is to treat the problem mathematically like a diffusion process, where the diffusion coefficient is adapted locally to the effect that diffusion stops as soon as an object boundary is reached [Per90].

5.6.7 Metal Artifact Removal Filter

An algorithm to reduce metal artifacts from dental filling was tested in this thesis. The algorithm first identifies the affected regions on each slice using mathematical noise estimation. This is based on the assumption that gray value levels areas that are affected by metal artifacts are significantly higher than anywhere else in the image. Once the affected areas are identified a 3D non-linear interpolation is performed in the spatial domain in order to remove the detected artifacts. The advantage of the approach used here is that ensures conservation of information because any non-affected data will not be filtered. Moreover it is computational fast and takes morphological features into account since this algorithm works in the spatial domain.

5.7 *Visualization*

This chapter introduces the three visualization techniques for tomographic images used in this thesis: the plain 2D slices, 3D volume visualization and 3D surface models The techniques were reviewed and criteria were formulated not only for visualizing the original patient scan but also how visualization techniques can be applied for the segmentation process.

5.7.1 General Aspects

Visualization of tomographic images is complex since three-dimensional volume has to be visualized on a 2D film or screen. Printing slices of the particular volume next to each other is well known and established for CT and MRI images, however this truly 2D visualization makes it sometimes hard to clearly identify related structures that are presented in many subsequent slices. Especially in cranio-facial surgery relations of bones that further apart are important for the outcome of certain interventions. Possible solutions are resliced 2D images in perpendicular orientation or a 3D representation where the whole skull can be easily inspected. Apart from the diagnostic visualization, for segmentation the problem is even more complex since for segmentation two data sets have to be visualized. First, the original data set that contains the anatomical and pathological information. Second, a label data set that stores the segmented structures as labels. These can be thought of as a transparents laid over the original CT scan on which structures of interest are marked with a crayon. Different labels can than be assigned to different anatomical and pathological structures (e.g. red for artery, green for tumor).

So far most software packages employ a 2D visualization technique to visualize these two data sets [AMI, ANA, MIM, SLI]. That is using overlay planes that visualize the label maps laid over the original data set on 2D slice views (see Figure 18). The approach presented in this thesis is based on a 3D representation of the label and original dataset. After segmentation 3D surface rendering is possible and has the advantage of being computationally fast and therefore interactive. This permits manipulation of the 3D scene and is commonly used for computer-aided surgical planning.
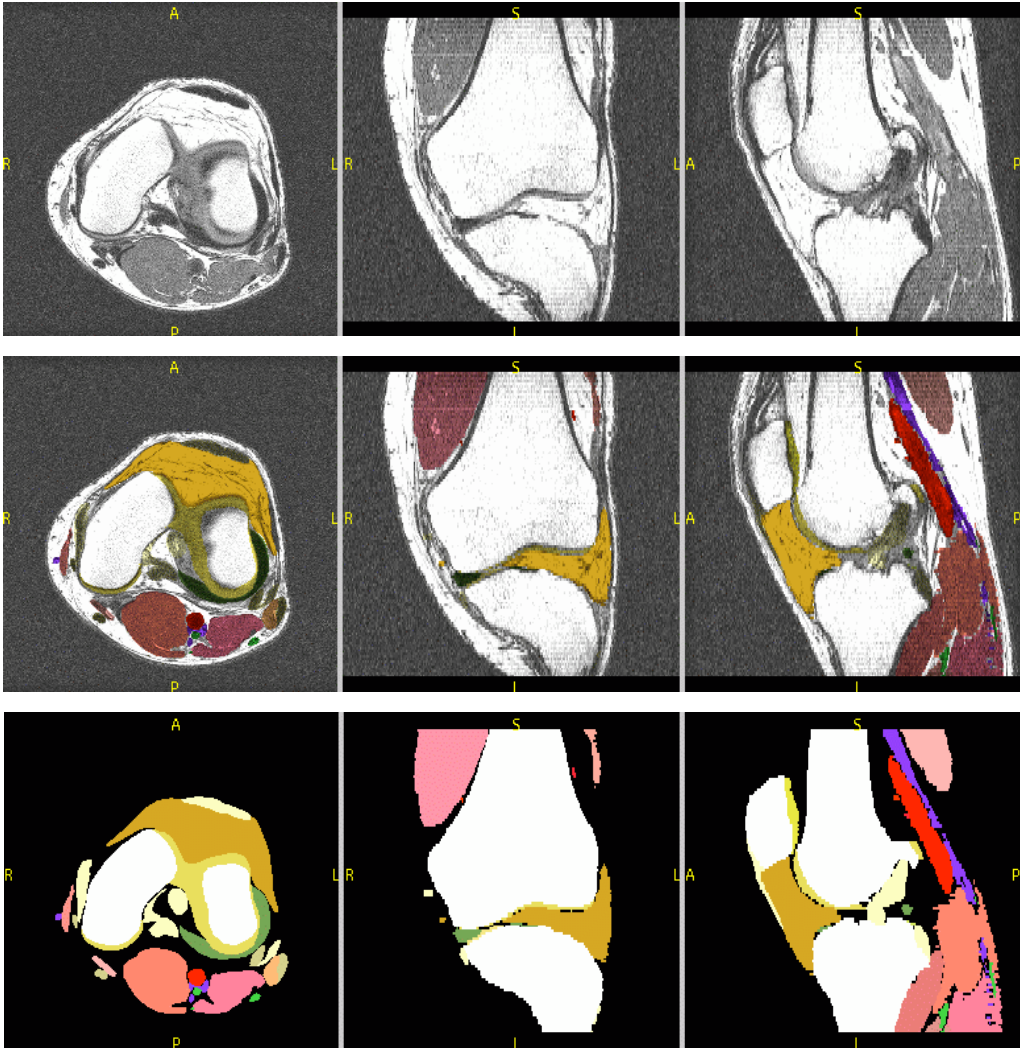

Figure 18: MRI data set of a knee and its segmented label map in three perpendicular views: axial, sagittal and coronal. Top row: unaltered data. Middle row: segmented label data overlaid on the original data set. Bottom row: label data only [SPL].

5.7.2 2D Visualization

2D visualization refers to the well-known concept of displaying tomographic images as 2D cross-sectional slices of the patient anatomy. Using computers one can easily reconstructed 2D slices in any given orientation. Common used orientations are axial, sagittal and coronal views. Since for CT images the resolution in the plane that the data was acquired is much higher than in any other orientation, resolution is much lower when such orientations are reconstructed (see Figure 19). However, for inspection of anatomical structures this can be very helpful sometimes. For segmentation three perpendicular slice views of the scan help to control algorithms that are applied to the whole volume. Thereby one can see at least in three different orientations how the algorithm works. Nevertheless, only three sections at a time can be seen and not the whole volume. To inspect the remaining sections one has to scroll through the orientation of choice and inspect the other slices. This can be very time consuming considering the increasing resolution of modern CT scanners and the large resulting number of slices. For abdominal scans several hundred slices are common, stressing the need for efficient visualization techniques.

The ability to reconstruct any given slice through the volume has certain advantages, for example if one places the slice along the axis of an anatomical structure. However these views are difficult to interpret and are not used that often.
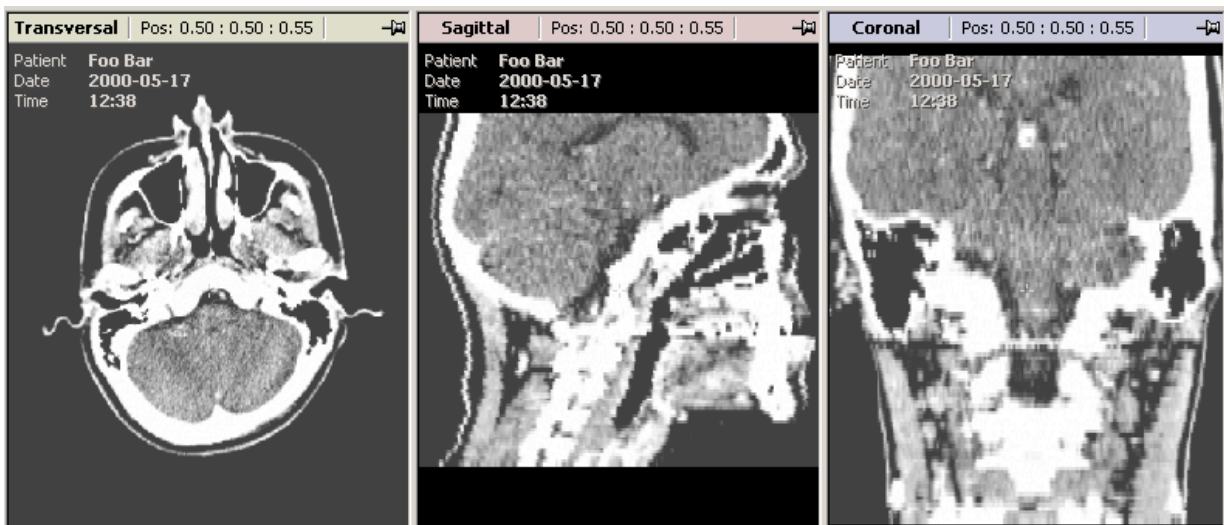

Figure 19: Perpendicular views of a axial CT scan of the head 320x 320 pixels. Note the decreased quality in the Sagittal and Coronal view due to resampling.

The great advantage of 2D slice visualization is speed. Since only one 2D slice or to the max three 2D slices have to be displayed and no computational intense operations have to be performed, one can quickly manipulate views and scroll through slices.

5.7.3 3D Volume Visualization

When adding slices of a tomographic data set with known dimensions to a stack of slices one can calculate a volume. Computer graphics techniques can be used to calculate 3D renderings of a volume.

The earliest volume visualization method is known as the maximum intensity projection (MIP). Along a set of virtual rays of projection that cross a given volume dataset the maximum intensity value in the volume is projected on the viewing plane (i.e. the screen). This technique is particularly useful for the visualization of tomographic scans derived from angiographies since the contrast agent filled vessels significantly differ in gray values from the rest of the scan. The ray-casting approach works similar but arbitrary portions of the volume content can be highlighted by the projection ray passing trough the volume towards the viewing plane. Therefore other than the highest gray values can be emphasized and displayed. Using this technique one can easily generate 3D volume renderings of different anatomical structures.

3D volume rendering has proven to be useful for the display of original patient data since it visualizes complex spatial relations of the anatomy in an intuitive fashion. However, so far only few reports are given in the literature of applying this method for displaying label maps. One reason for this has been the computer hardware performance. Medical CT scans can be very large and the whole volume has to be stored in the working memory of the computer in order to provide interactive display. Adding another label map volume exceeded hardware capabilities of common personal computers (PC) in the past and were only possible using high-performance computer not available in most hospitals. Today new graphic cards are available that can handle such large data sets and interactivity can be provided on a standard PC.

5.7.4 3D Surface Visualization

As a prerequisite to generate 3D surface models, the boundaries of the structures of interest on a given data set have to be defined and stored on a label data set. Different segmentation algorithms, as explained below, can be used for this task. The output of the segmentation is a binary label data set where the structures of interest are represented by different labels.

To generate a surface from these labels, a surface reconstruction algorithm has to be applied. The marching cubes algorithm has proven to be very robust and efficient [Lor87] for this purpose. This algorithm calculates for a given iso-surface value a triangle surface. First, eight direct adjacent voxels within the volume are considered as a cube. This cube traverses the whole volume (i.e. the marching cube). The value at the corner points of the cube determines, whether this particular point is "inside" or "outside" the desired structure to be extracted. This value is user-defined and for binary images resulting from segmentation either one for inside the structure or zero for outside the structure. The generated surface intersects those edges of the marching cube where one vertex is inside and one outside. By linear interpolation within the cube edge, the actual point of intersection somewhere between the two vertices is calculated. This implies for surface reconstruction from binary volumes, that this interpolated point will always be exactly in the middle of the two vertices disregarding the information content of the original gray value image where "real" interpolation would have been possible.

Once such a surface has been reconstructed the 3D surface model can be displayed and inspected from any angle. Since only surface have to be displayed which consist of triangles, the visualization is computationally very effective and real-time manipulation of the model is possible as opposed to 3D volume rendering.

5.7.5 Criteria For Efficient Visualization

Visualization of the segmentation process has several tasks to fulfill. First it has visualize the underlying original dataset that is to be segmented, second the label data set has to be displayed showing the current status of the segmentation. Ideally, the user could see the whole volume at a glance and as soon as one changes parameters of the segmentation algorithm the volume should be updated in real-time. Additionally to the volume view, one needs to be able to inspect a given slice to check for details of the segmentation and these two views should be easily correlated (i.e. indication of the slice in the volume rendering). One should able to toggle the visualization of the label dataset in order to inspect the original dataset in detail and different opacities of the label dataset should be available. Center and width of the original gray values of the CT scan should be adjustable in real-time.

Following these criteria the user interface for the 3D interactive segmentation was designed.

5.8 Image Segmentation

This Chapter gives a brief overview of some common aspects of segmentation of medical images and a possible classification of segmentation algorithms. Region grow, threshold and manual segmentation as common segmentation algorithms used for bone segmentation from CT images are introduced. Differently visualized threshold segmentations were tested. Manual segmentation of each dataset was performed to server as a reference for the various threshold segmentations.

5.8.1 General Aspects

The principal goal of segmentation is to partition images into regions that are uniform for one or more characteristics or features. Segmentation in medical image processing in that sense refers to identifying anatomical, pathological or any structure of interest on a medical image.

Segmentation methods can be classified by many aspects [Ban00, Pal83]:

- Manual, semiautomatic and automatic
- Pixel-based (local methods) and region-based (global methods)
- Manual delineation, low-level segmentation (threshold, region growing, etc.) and model based segmentation (mulitspectral or feature map techniques, dynamic programming, contour following, etc.)
- Classical (threshold, edge-based and region-based techniques), statistical, fuzzy and neural network techniques.

In order to achieve the best results when segmenting, the used method should be chosen carefully considering the desired segmentation target as well as the imaging modality. Very sophisticated fully automatic segmentation algorithms exist but they often work not reliably for any data set and obviously not for any given pathological anatomical structure. Moreover, for some of the automatic algorithms difficult parameter tuning is required and performance can be very slow (i.e. several hours to segment one data set). Therefore semi-automatically

algorithms were evaluated in this thesis. Since this concept involves user interaction, special attention during the development of such algorithms has to be drawn towards efficient user interfaces. In this regard visualization takes an important role.

The most commonly used algorithm for bone segmentation is threshold [Wes98]. It can be considered as a region-based segmentation techniques as opposed to edge-based techniques. The former looks for regions satisfying a given homogeneity criterion while the latter looks for edges between regions with different characteristics.

Manual segmentation refers to outlining structures by hand. While this technique is not very efficient, it is still commonly used, since other segmentation methods that might have been applied to a particular dataset still need manual refinement. For some structures there exist no automatic or semiautomatic algorithm at all, leaving manual segmentation as the only choice.

5.8.2 Threshold Segmentation

Threshold segmentation is to distinguish pixels within an image by their gray value. The distribution of gray values in images can be visualized as a histogram of either gray values or Hounsfield units in x-axis and quantity in the y-axis (see Figure 20). Given this distribution a threshold can be applied to one image or region or the whole data set. An upper or lower threshold can be defined, separating the pixels into structure and background (i.e. all pixels above the given upper threshold are no further considered and visa versa for the lower threshold). However, when the corresponding histogram modes of different structures overlap, it is very difficult to find a satisfying global threshold. This problem can be partially addressed by image enhancement algorithms like the Markov random fields filter as this operation homogenizes areas to a certain degree (see Chapter Image Enhancement).

As gray values correspond to the density of the imaged structures in CT, this approach is suitable for identifying bones. Bones are highly radio dense compared to soft tissue. This makes it reasonable to find a threshold within a
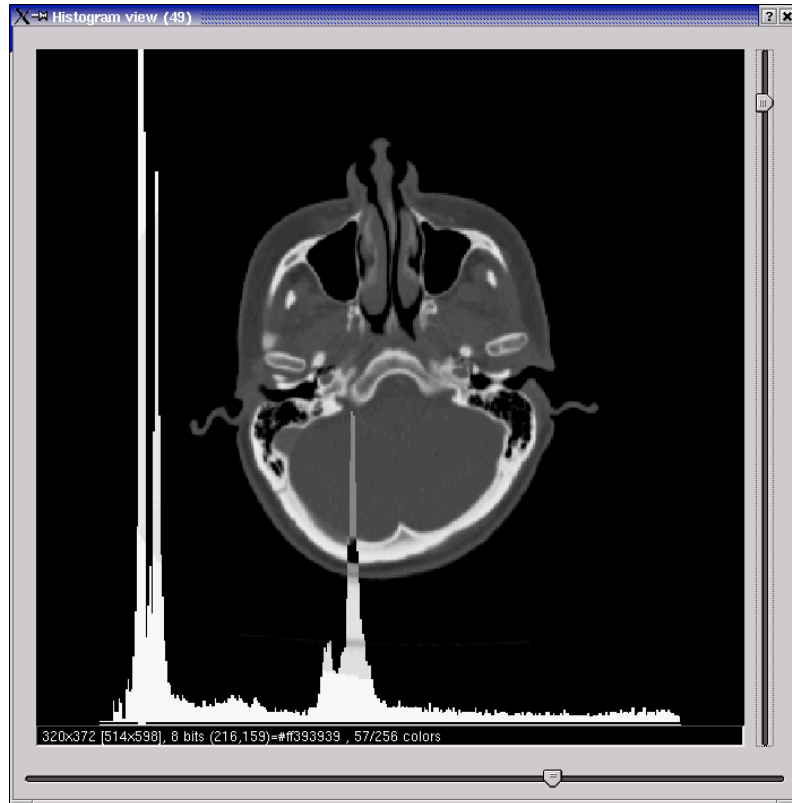
Figure 20: The histogram shows the gray value distribution of the underlying CT slice. On the X-axis the intensity values are dRawn while on the Y-axis the number of incidence for each gray value is portrayed.

global gray value histogram of a CT that distinguishes bone from other tissue. Therefore threshold algorithms are commonly used for the segmentation of bone as in this thesis. Once values are chosen, the segmented volume can be calculated very quickly even for very large data sets. This information is then stored in a label data set.

However, due to the partial volume effect on very thin bones (e.g. walls of the maxillary sinus) or the very small distances between neighbored bones (e.g. joints) under run spatial resolution capabilities of the certain scanners, threshold segmentations do not always yield sufficiently accurate results. Image enhancement algorithms can achieve some improvement but subsequent manual refinement taking approximately one to two hours is often necessary [Eve00].

5.8.3 Region Growing Segmentation

Whereas threshold focuses on the difference of pixel intensities, the region growing method looks for regions of pixels with similar intensities. First, a starting or seed point for the algorithm is chosen within the region that is to be segmented. This is usually done manually but can also be performed by an automatic seed point technique. From this point the algorithm for similarity based on a homogeneity criterion investigates all neighboring pixels. If the criterion is fulfilled the particular pixel is added and its neighbors are tested. This procedure iterates until no more pixels can be added. All identified pixels then represent the segmented object [Ada94]. One example for the homogeneity criterion is to compare the difference of intensity values of a particular pixel to the mean intensity value of a region. If the difference is less than a predefined value, for example one standard deviation of the intensities across a region, the pixel is added to the region. The region growing approach can be applied on a 2D and 3D basis. Since tomographic scans represent a volume most region growing algorithms for medical images are working on a 3D basis.

The results of a region-growing algorithm strongly depend on choosing an appropriate homogeneity criterion. If the criterion does not match intensity differences in the underlying picture, the algorithm will fail to identify regions belonging to one group of pixels. To set this problem under manual control interactive region-growing algorithms were developed that allow the user to tune the homogeneity criterion and display the resulting segmentation as an overlay on the slice in real-time.

5.8.4 Manual Segmentation

Manual segmentation refers to outline structures of interest within a radiological image by hand. The tools used for that usually include a painting brush known from standard painting software (e.g. Microsoft Draw etc.) in various sizes, filling tools, polygon drawing tools or similar. However, manual segmentation is a very labor-intensive task given the number of slices usually present in a CT data set.

The user has to inspect each single slice and segment the structures of interest. Despite the simplicity of these tools there are still indispensable for segmentation problems so far. Often the semiautomatic tools need manual refinement for sufficiently accurate segmentation. Moreover, manually segmented datasets by experts can serve as reference to test newly developed algorithms against. This strategy was chosen to evaluate the segmentation method introduced in this study
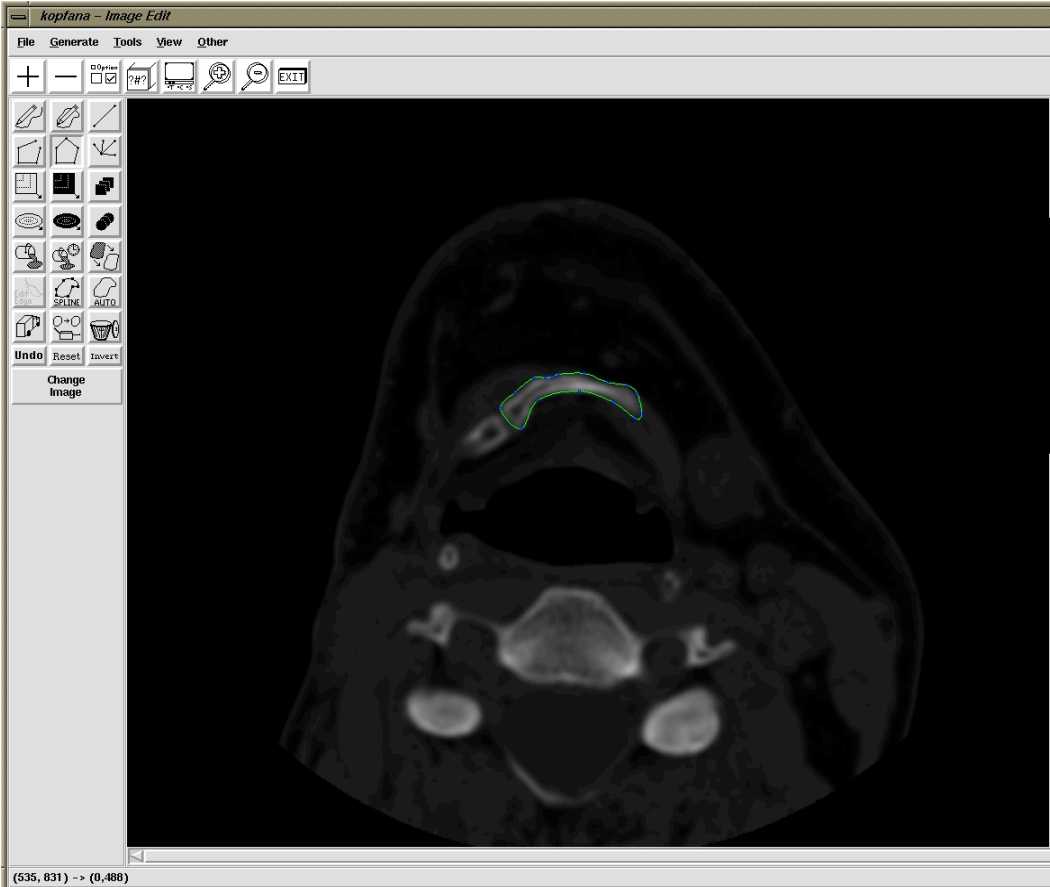

Figure 21: The Analyze user interface for manual segmentation. On the left different tools for changing slice, zooming, filling and painting can be chosen from a toolbar. These can be applied to the particular slice shown on the right, where parts of the mandible were manually outlined.

5.9 Evaluation of Segmentation Algorithms

This chapter explains the methodology used for evaluating the new 3D interactive threshold segmentation approach regarding accuracy and efficiency. The 3D interactive segmentation was compared to 2D threshold and manual segmentation. First, the general procedure is outlined, and then the used statistical methods are elucidated.

5.9.1 Procedure

3D surface models according to the above outline procedure (i.e. image enhancement, segmentation, 3D model reconstruction) of all seven cranial CT scans were generated using

     a. 2D interactive threshold

     b. 3D interactive threshold

     c. Manual segmentation.

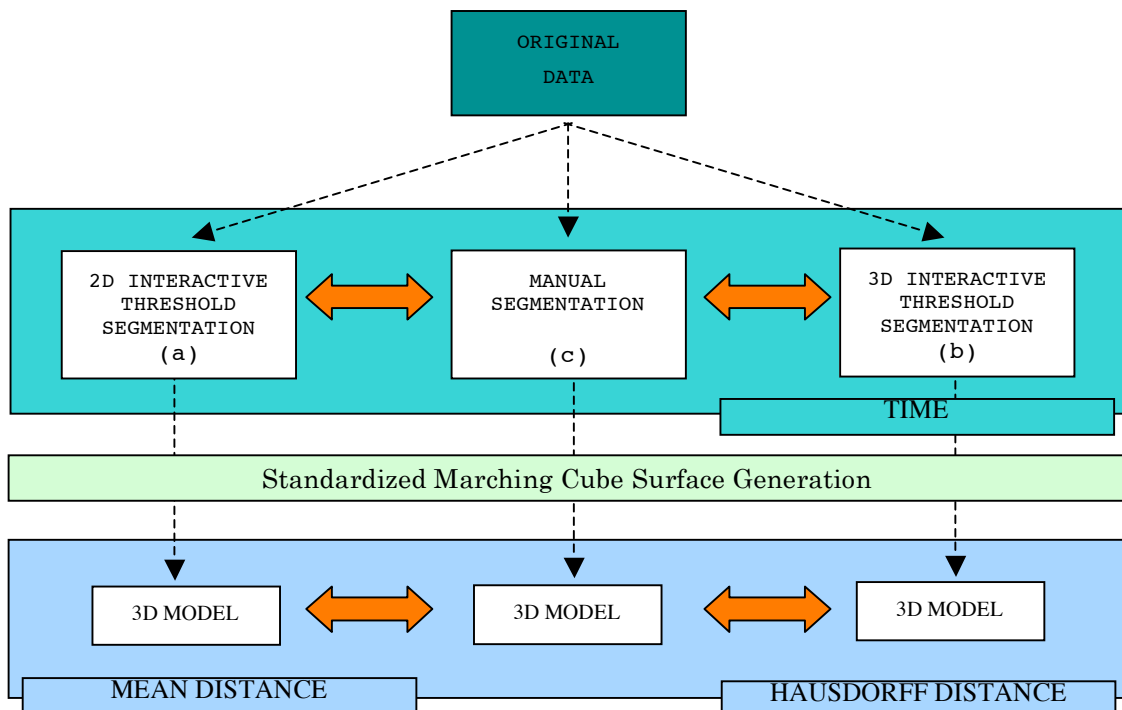Prior to segmentation, all datasets underwent exactly the same preprocessing

Figure 22: Outline of the study design to assess accuracy and efficiency of the evaluated methods by time comparison of the segmentation task (top row). After standardized surface reconstruction mean and Hausdorff distance for the particular 3D model were calculated. Orange arrows show comparisons while the dashed arrows outline the subsequent processing steps of the data.

steps of Markov random fields based filtering and metal artifact removal as explained above.

Efficiency was evaluated by measuring the time needed for each segmentation. Times for 2D (a) and 3D (b) visualized segmentations as well as manual segmentations (c) were then compared (see Figure 22).

Accuracy was assessed by calculating the mean and the Hausdorff distance of 3D surface models derived from 2D and 3D visualized segmentations as well as comparing them to a manually segmented dataset taken as a reference (a vs. c, b vs. c). For calculating the Hausdorff and mean distance, a special evaluation module for the software framework Julius was developed and used for this thesis.

5.9.2 Hausdorff Distance (Maximum Surface Distance)

The Hausdorff-Chebyshev metric defines the largest difference between two surfaces or contours. Given two contours C and D, first the minimal distance for each point c on C is calculated to all the points on the contour D:

$$d_C (c,D) = \min \{ d_{PS} (c,s), s \subset D \}$$

Then this minimal distance is calculated for each boundary point and takes the maximum minimal distance as the "worst case" distance:

$$H_C(C,D) = \max \{ d_C (c,D), c \in C \}$$

The Hausdorff metric is not symmetric and $H_C (C,D)$ is not equal to $H_C (D,C)$, which is accounted for by finally calculating:

$$H_C(C,D) = \max \{ h_C (C,D), h_C (D,C) \}$$

However, the Hausdorff metric calculation is computationally very expensive as each contour point to all the others is compared. Therefore the calculation was simplified as a 3D Euclidian distance transform calculation on one object and overlay of the second was used to efficiently calculate the measure [Ger01].

5.9.3 Mean Distance

The mean distance represents the average of all smallest distances between two surfaces.

$$\text{Mean of } X = \mu = \sum_{l=1}^{n} p_l X_l \text{ , for N values of X}$$

$$= E\ (X)$$

For each point of the surface model representing the manual segmentation the smallest distance to the surface model to be compared (i.e. models derived from 2D and 3D visualized segmentations) was measured. The distances for all points were added and divided by the number of points on the original data set. This was repeated for each data set.

6 Results

In this chapter results are presented for each processing step involved in the proposed processing pipeline. The accuracy and efficiency evaluation of the newly introduced 3D interactive segmentation algorithm as the central part of the evaluation is presented in detail.

6.1 *Data Management*

For this thesis the image data was initially copied from MOD's to CD's and transported from the radiological department to the surgical planning site. Copying from MOD's was achieved using the inherent scanner software. CD's were either send by mail or were picked up in person.

A digital Dicom server connection between the department of radiology and the surgical planning site at the research center caesar was then established. This enables us now to transfer images digitally from the clinic of craniofacial surgery in Munich to the research center caesar. The software Pmod [PMO] and two dedicated computers were acquired for this purpose. The computers had to be placed outside the firewalls of each involved institution and were equipped with a RAID hard-disk system. This hard-disk system secures the data saved on it even if one of the hard disks breaks down. Placing the computers outside the firewall made use of the Dicom server more secure for the institutions. To connect to the Dicom Server only listed IP addresses are permitted only at certain ports. Thereby security for the Dicom server was guaranteed. From the inside network of either institution a secure shell tunnel was established to access the data from its Dicom server. Finally the server worked and facilitated further data transfer between the two institutions

The data was in Dicom 3.0 format and was imported into the Julius software framework. Due to varying standards of Dicom 3.0 some software modifications of the Dicom reader in Julius had to be done in order to read data correctly.
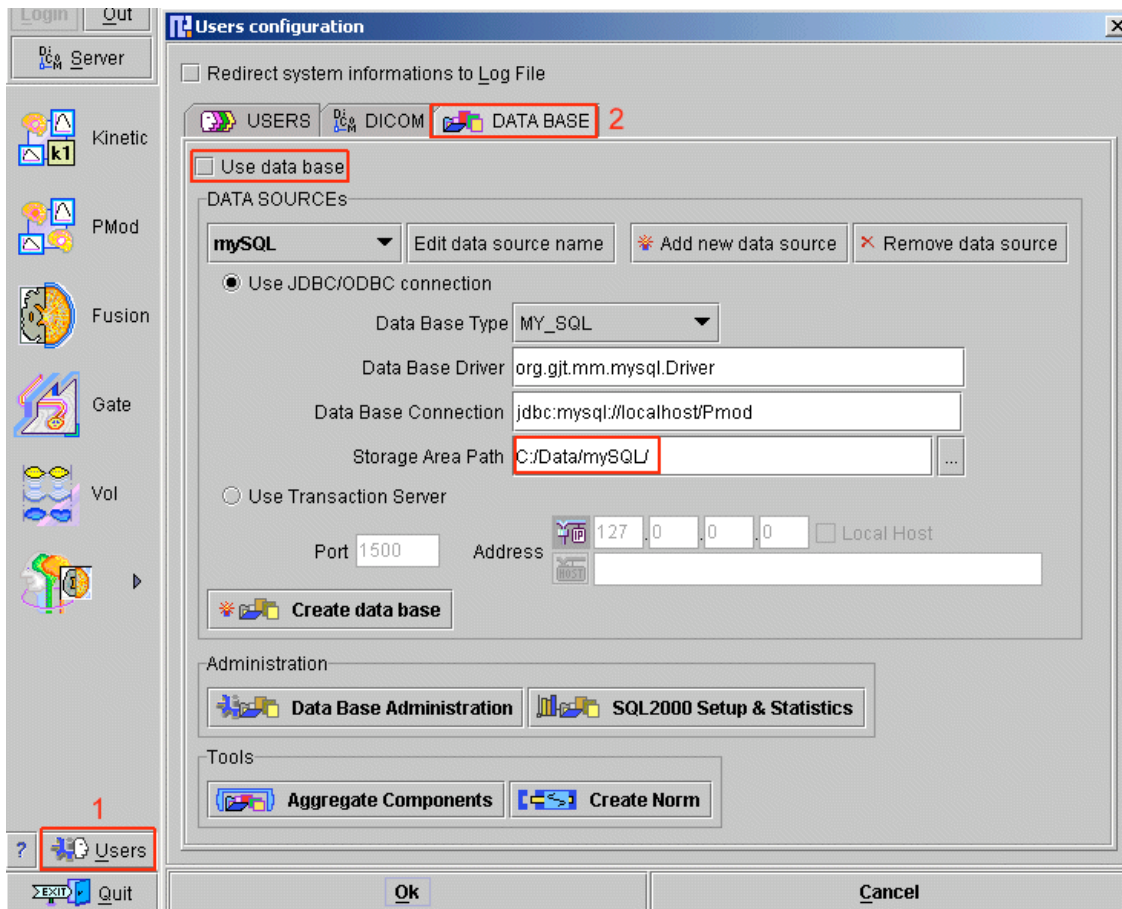

Figure 23: Pmod user interface for data transfer by the Dicom server.

Julius was also used to convert the original Dicom format into Raw format for two reasons: First, by the time 3D Slicer was tested it could not read Dicom images. The second reason was the initial implementation of the 3D interactive segmentation module that was capable of reading Raw images only.

Several issues had to be respected when converting from one format to another: First it has to be sure that during the conversion no information is lost or altered. Especially the information related to spacing and pixel size is prone to errors, since vendor specific definition of these variables may vary. Visually comparing the data and performing measurements on the original and converted data sets and comparing them achieved this.
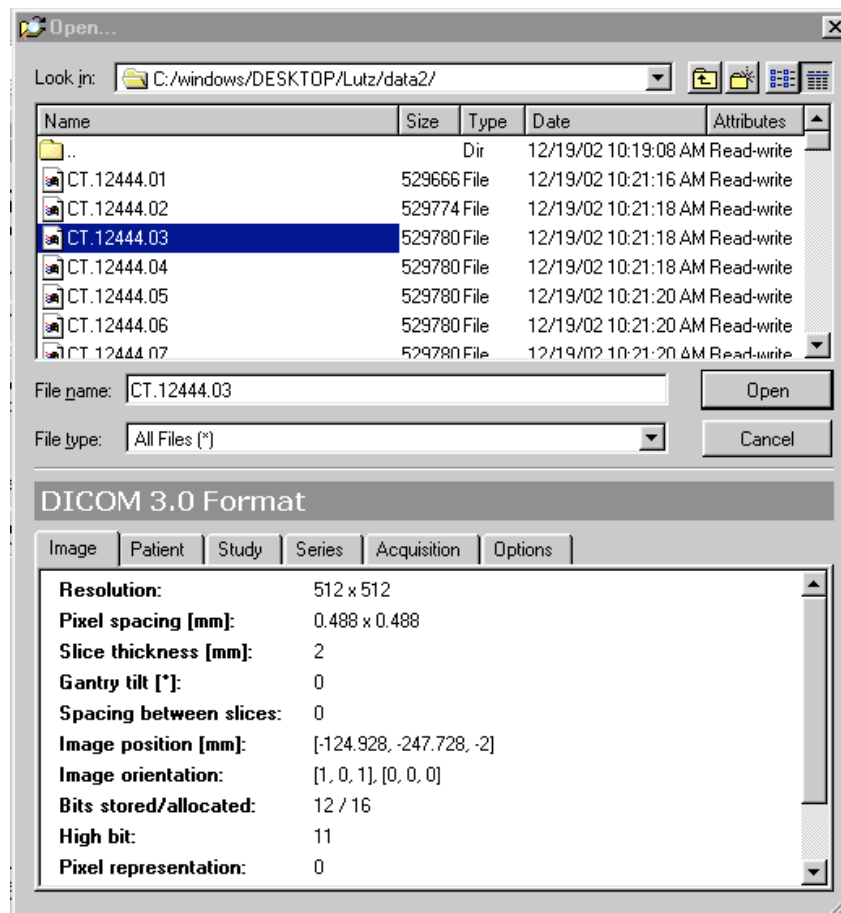
Figure 24: Open file dialog of Julius. By clicking on one of the files, the user receives all important information in the lower part of the window. By activating the different step cards (below DICOM 3.0 Format) one can gather the different aspects of the information.

Another problem is that images are stored differently in UNIX and Windows machines: the so called little and big endian parameter is altered between the two systems: as outlined above the images are stored using 16 bit or 2 bytes. The position of the 2 bytes is flipped from little (i.e. smaller byte in front) to big (i.e. bigger byte in front) endian.

In order to improve data management further a new user dialog for loading data was designed (See Figure 24). Now, by clicking on one file of the data, the user can easily apprehend the most important information of the data set as patient name, number of slices, resolution, study date etc.

6.2 Image Enhancement

Several image enhancement algorithms were tested for the filtering of CT images in regard to subsequent segmentation. Results for each tested algorithm are listed here. The Markov Random field algorithm was found to be most suitable for the specific purpose of this pipeline and is along with the dedicated metal artifacts removal algorithm described.

6.2.1 Low Pass Filtering

Low pass filtering was applied to CT scans of our patient database using several options. The resulting images were visually analyzed. As an example the image in Figure 25 was filtered twice using a low-pass operation with a kernel size of 3 x 3 x 1 pixels. As shown this operation reduces noise in an image but at the expense of the blurring edges – in this case the translation from bone to air. This is especially unpleasant when one tries to segment exactly this edge by a threshold algorithm. The filtering operation was accomplished rather fast, but parameter tuning can greatly vary the resulting filtered image. Even with constant parameters results differed among different data sets. For the purpose of this thesis a reliable and as constant as possible filtering algorithm was anticipated in order to standardize this part of the processing pipeline. Therefore the low pass filter was not found to be suitable to be integrated into the proposed processing pipeline. However, the low pass filter worked reliably and for removing noise for visual inspection it can be used within its limits.
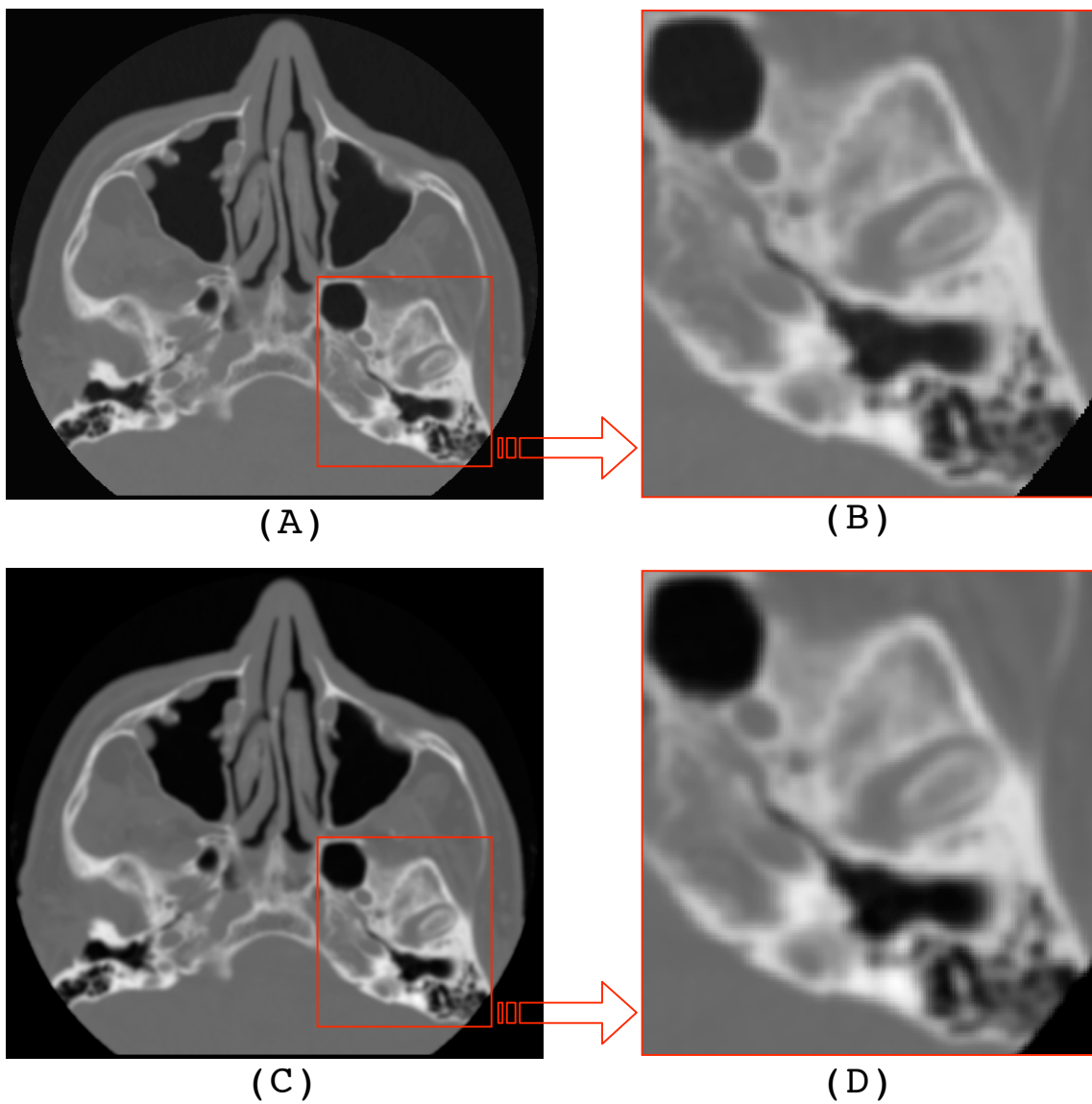
Figure 25: (A) shows the original, unfiltered Slice of a cranial CT scan, 512 x 512 pixels, 0,82 x 0.82 x 3 mm voxel size. (B) The red marked area zoomed by a factor 3. (C) Shows the same image low pass filtered twice with a kernel of 3x3x1 voxels. Already in the unzoomed image one recognizes the slight smoothing in (C) which is stressed in the zoomed image (D) illustrating parts of the mastoid and the temporal-mandibular joint.

6.2.2 Median Filtering

This filter was also applied to CT datasets of our patient database and results were visually compared. The median filter was found to be less smoothing than the low pass filter. Noise could be diminished and edges were not smoothed as much but as can be seen in the example (see Figure 26) wrong chosen parameters can greatly impair performance. As shown in the example a relatively high z-axis value of 5 lets the filtering take the neighbored slices over-proportionally into account. The filter does not adapt as much as to the underlying image and is
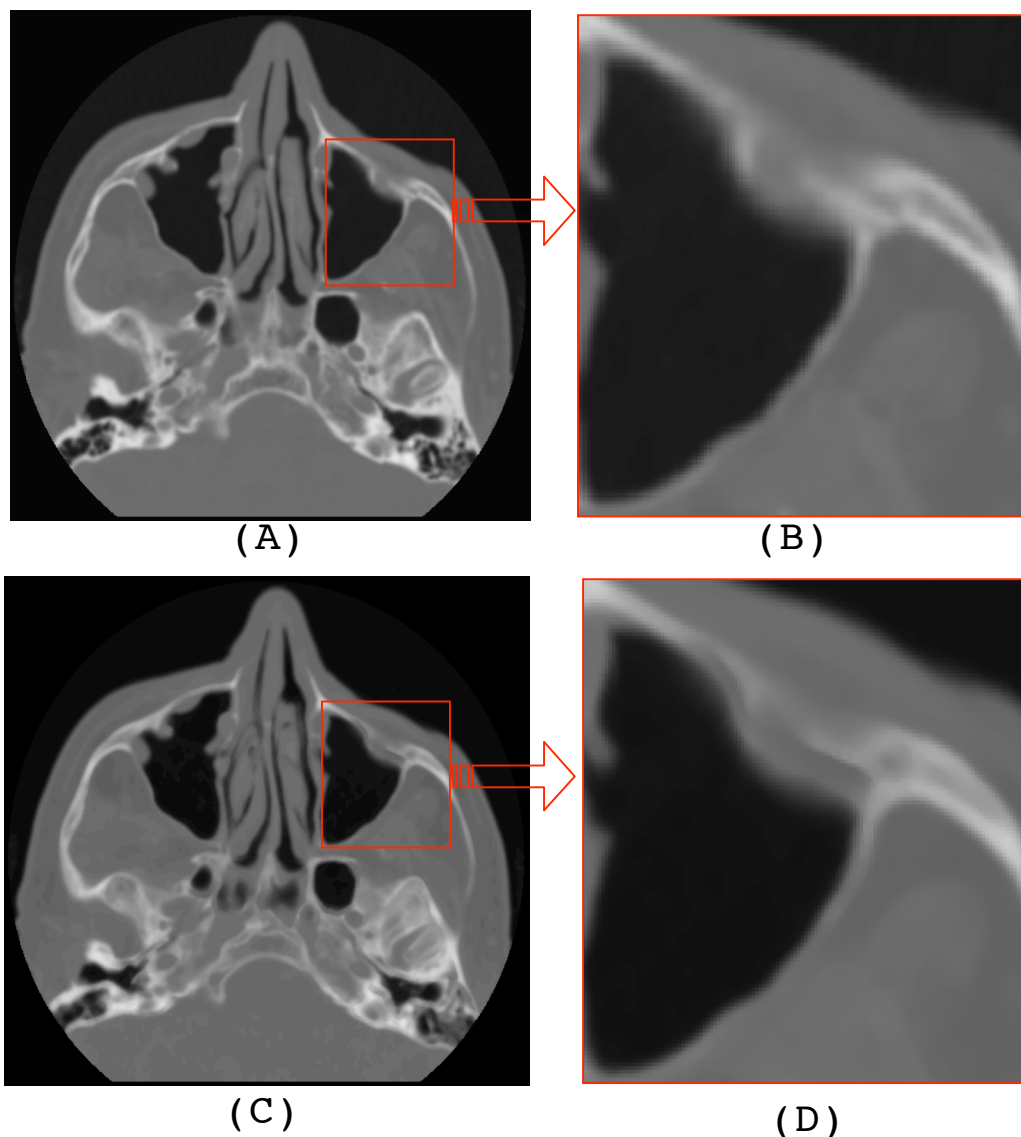

Figure 26: (A) shows the original, unfiltered Slice of a cranial CT scan, 512 x 512 pixels, 0,82 x 0.82 x 3 mm voxel size. (B) the red marked area zoomed by a factor 3.(C) shows the same image filtered with a median operation with a kernel of 3x3x5 voxels. Due to the kernel size the influence of the adjectant slices within the filtering becomes obvious. Blurring can be observed and the reduced gray value fluctuation within the cave of the maxillary sinus can be observed (C and D).

therefore sensible to parameter tuning when different datasets are to be filtered. For the sake of comparability this is a disadvantage.

6.2.3 Anisotropic Diffusion Filtering

The anisotropic diffusion filter was able to enhance edges and adapt to local image features. Parameters had nevertheless to be tuned, and were not very intuitive. Because one filter iteration can take up to 10 min (SGI Octane 2) this
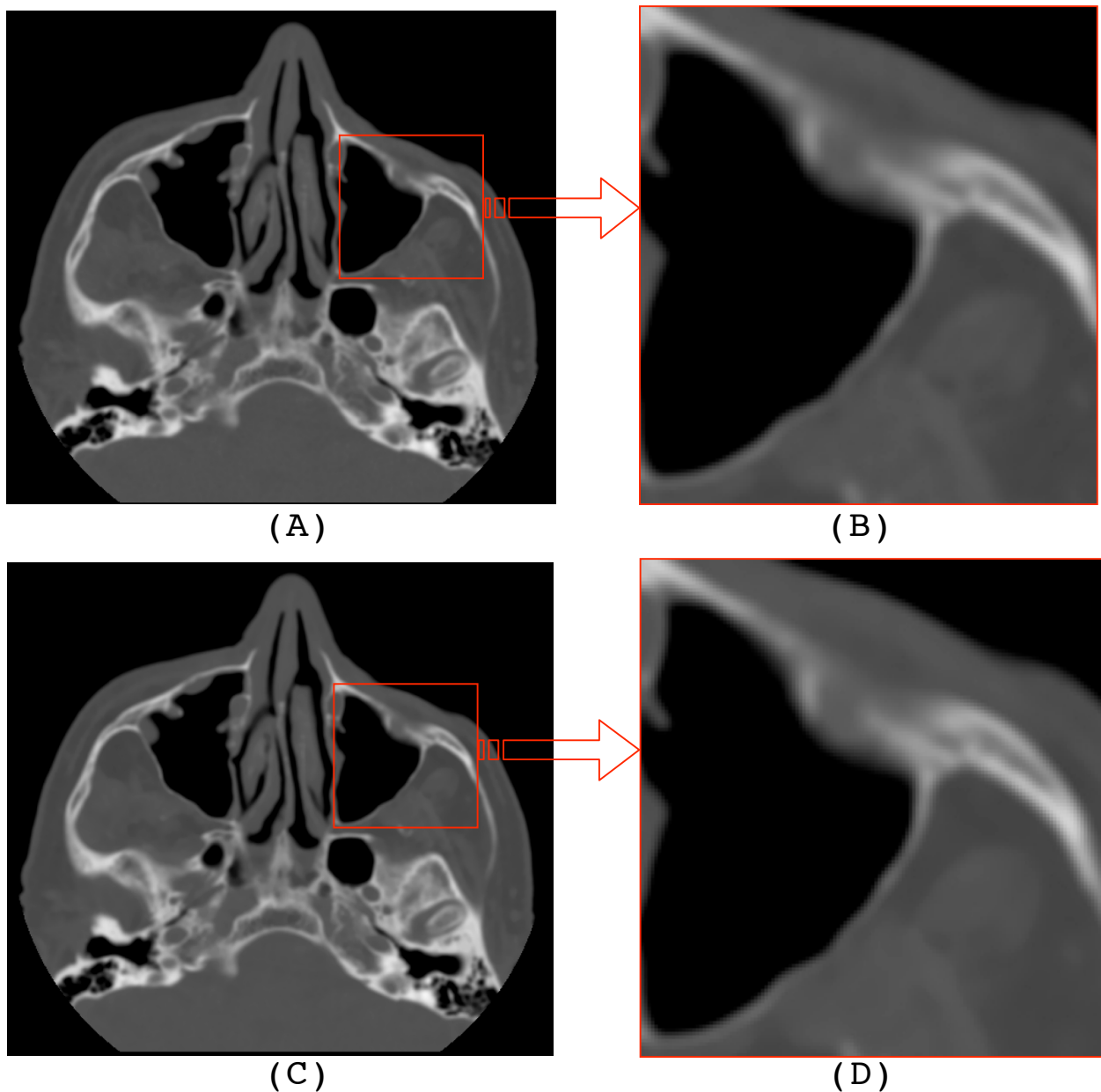

Figure 27: (A) shows the original, unfiltered Slice of a cranial CT scan, 512 x 512 pixels, 0,82 x 0.82 x 3 mm voxel size. (B) the red marked area zoomed by a factor 3. (C) shows the same image filtered with a anisotropic diffusion filtering. Edges are enhanced and the reduced gray value fluctuation within the anterior cranial fossa can be seen.

can be very time consuming. This method has two great advantages compared to the median and low pass filter. First, it filters the image while taking specific image features into account (i.e. adaptive) and it works in an anisotropic manner. Therefore the filter was able to respect unevenly distributed voxel sizes, but is still able to filter in a 3D space. The method appears to be suitable to effectively filter CT data sets for bone segmentation by threshold [Eve00]. Nevertheless certain parameters regarding the underlying diffusion process have to be tuned in order to obtain meaningful results. Maintaining these parameters constant for different CT data sets does not reveal sufficient filter images and therefore the subsequent comparison of different segmentation algorithms would have been severely hampered.

6.2.4 Markov Random Field Filtering

The Markov random fields filter was applied to all datasets and able to reliably remove noise and enhance edges. The main advantage of this filter lies in its statistical nature, leaving no parameter tuning to the user. Thereby all images could be filtered in a standardized way making the objective evaluation of subsequent processing steps possible. The filter respects anisotropic voxels sizes and statistically adapts to local image features. Filtered images appeared to have more contrast and the bony structures were to be distinguished much easier.
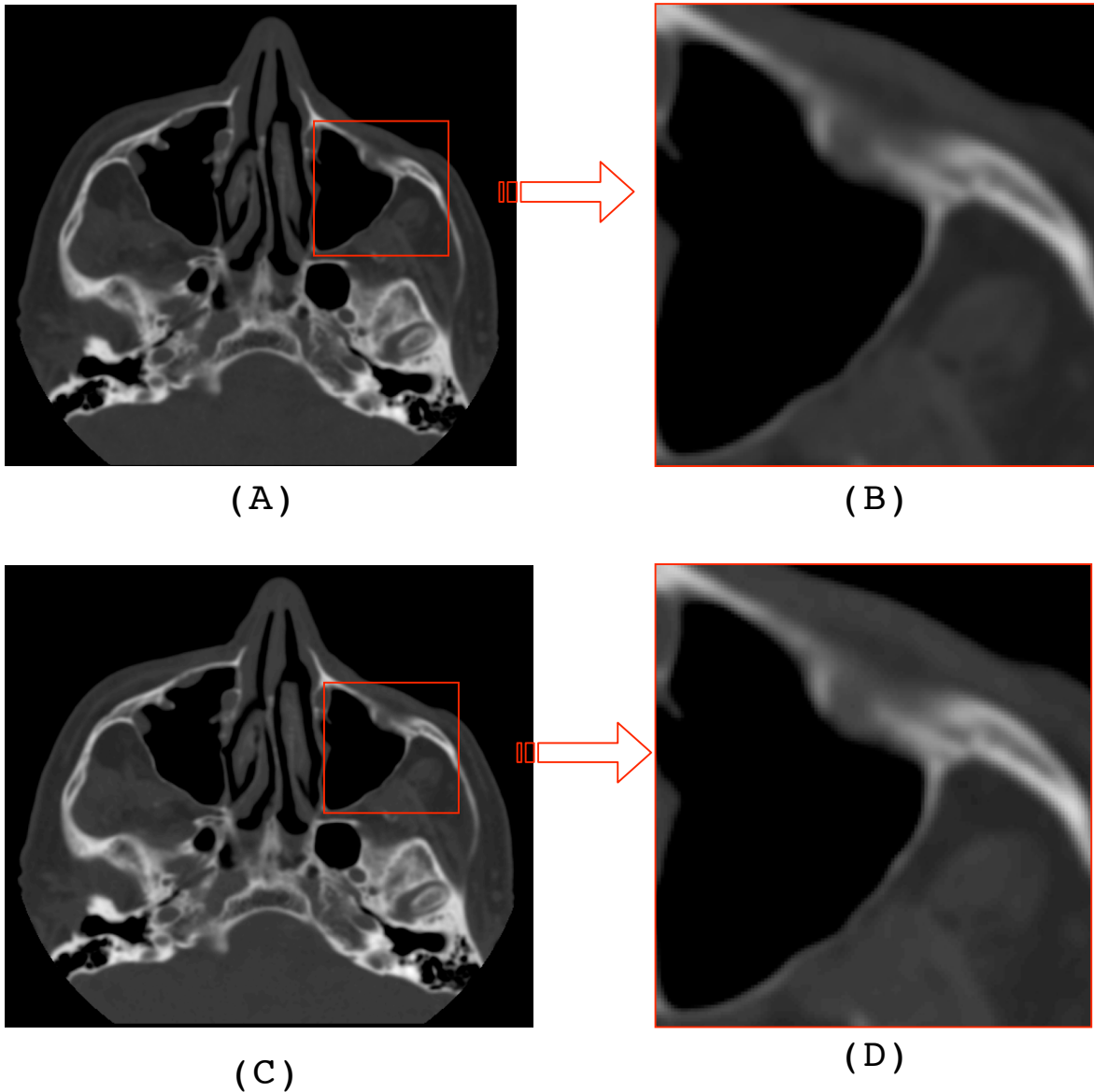
Figure 28 (A) shows the original, unfiltered Slice of a cranial CT scan, 512 x 512 pixels, 0,82 x 0.82 x 3 mm voxel size. (B) the red marked area zoomed by a factor 3. (C) shows the same image after a Markov Random Field filtering was applied. Note the enhanced bone edges on the zoomed image, as well as the grouping of the gray values within the anterior cranial fossa.

6.2.5 Metal Artifact Removal

All seven CT data sets were filtered with this algorithm in order to reduce metal artifacts commonly found in cranial CT scans.

Metal artifacts derive from the strong X-ray attenuation of implanted metallic prostheses, clips or dental fillings. Dental fillings are a common cause for dramatically impaired quality of cranial CT scans. One very straightforward approach to solve this problem is taking out what ever is causing the artifact and redo the scan [Odl01]. This method strongly depends on the indication and therefore cannot be applied for all cases. This study was performed retrospectively therefore manipulations on the patient were not possible, and not feasible either. Therefore a special image enhancement algorithm to diminish metal artifact was used for this processing pipeline. The algorithm greatly facilitated further segmentation by interpolating the artificial gray values derived from metal. For threshold and region growing segmentation this was very helpful, since bulky streaks in the subsequent 3D models could be minimized. However, for visual inspection or diagnosis the current stand of this algorithm appears questionable.
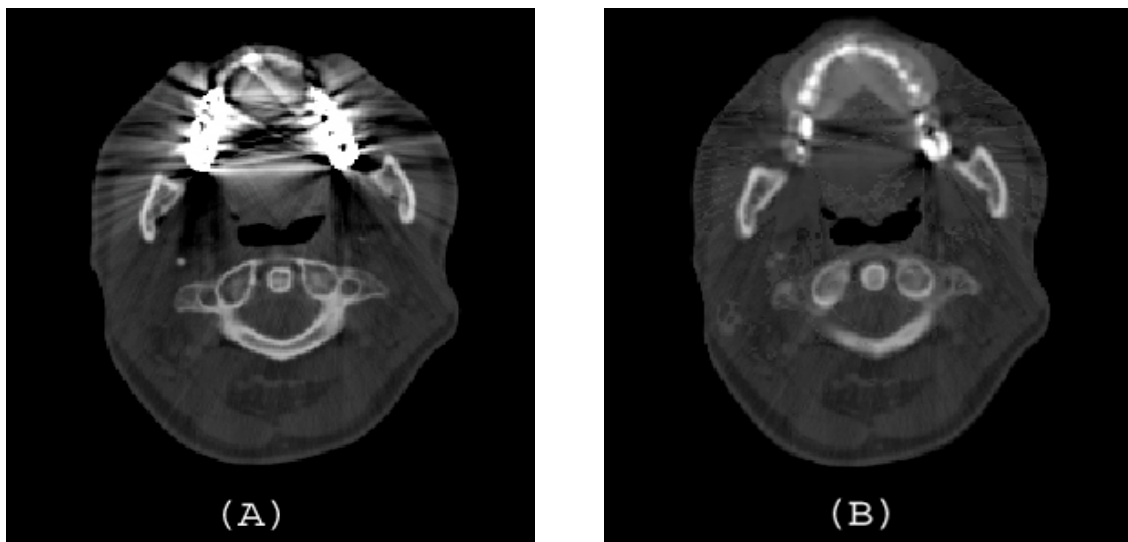

Figure 29 Axial CT slices before (A) and after (B) image enhancement consisting of metal artifact reduction and Markov random field based filtering.

6.3 Visualization

For 3D interactive segmentation a special volume visualization was implemented. Additionally, the marching cube surface reconstruction algorithm was used in dedicated way to reconstruct models for surface visualization.

6.3.1 Volume Visualization

Threshold, as a real-time volume visualized segmentation tool was implemented. This was embedded into the Julius user interface. After loading the data set the user can now manipulate the threshold value and view the segmentation results in real-time. Volume rendering by 3D texture mapping is used to display the volume data during interaction. Compatible with OpenGL, this technique allows real-time volume rendering: slices of the volume are directly rendered from back to front. An update rate of 10Hz is reached for a display size of 600x600 pixels to visualize volume-texture data of 512x512x128 voxels on SGI workstations, i.e. Octane2 and Onyx 3200 IR3. To enhance depth and iso-surface perception, soft shading (i.e. rendering technique) has been added without reducing the rendering time. This technique allows also superimposition of generated surfaces on the original (or segmented volume) for visual inspection.

Moreover the scene can be inspected from any angle and the three known perpendicular views, axial, sagittal and coronal, of the original data set with the segmented parts shown as overlays can be appreciated on the bottom on the screen. The tool was connected to an anatomical list in Julius that provides the entire anatomical nomenclature. The idea is to guide the user, who picks an anatomical structure and Julius starts the recommended segmentation algorithm. After the segmentation the user can then easily correlate the picked anatomical name with the segmented region on the image by clicking on it. In this case Julius proposes to start the Markov random field filtering algorithm once the user picks a bony structure of the skull. After filtering it opens the user interface of the 3 D interactive segmentation. Once the user confirms the finished segmentation, Julius starts the 3D reconstruction
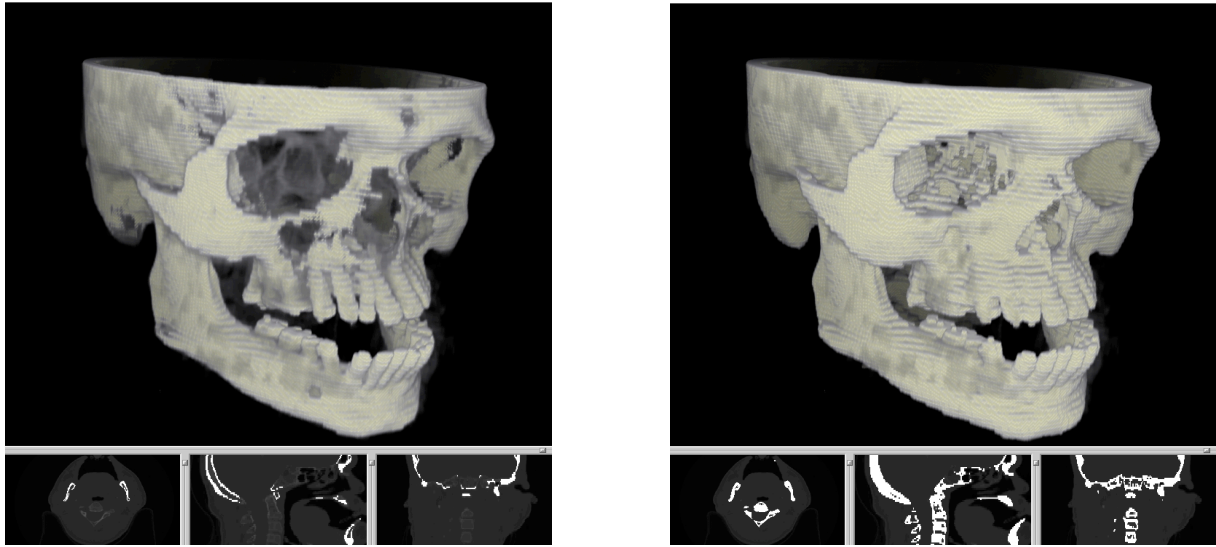
Figure 30 Screenshots of segmentations with the 3D texture mapping view and with the axial, sagittal and coronal slice view below is shown. Note the segmented parts displayed in lighter gray in the 3D scene compared to the yet unsegmented in darker gray. Progress by parameter tuning is shown from left to right for threshold segmentation.

.

6.3.2 3D Model Reconstruction

The marching cubes algorithm by Lorensen and Cline [Lor87] was modified to reconstruct 3D surface models for this thesis. The algorithm was customized to produce bone surfaces directly from threshold segmentations by taking the user defined threshold values for calculating surfaces into account. The main difference of this approach to the ones described is that the marching cube algorithm now interpolates between the user defined gray values considering all information from the original data set as opposed to take only binary information from a label data set into account. Using this approach one can demonstrate fine detail on the final 3D surface model. The marching cubes algorithm then produced an initial surface model consisting of several thousand triangles. To further improve performance a special algorithm reduces the number of triangles of the initial data set, hidden for the user, as far as possible [Kee97]. Thereby, fewer triangles have to be displayed for one model and the visualization can be calculated faster. Using Julius one can decide whether to emphasize more the original data set or to further interpolate and receive a smoother model in three
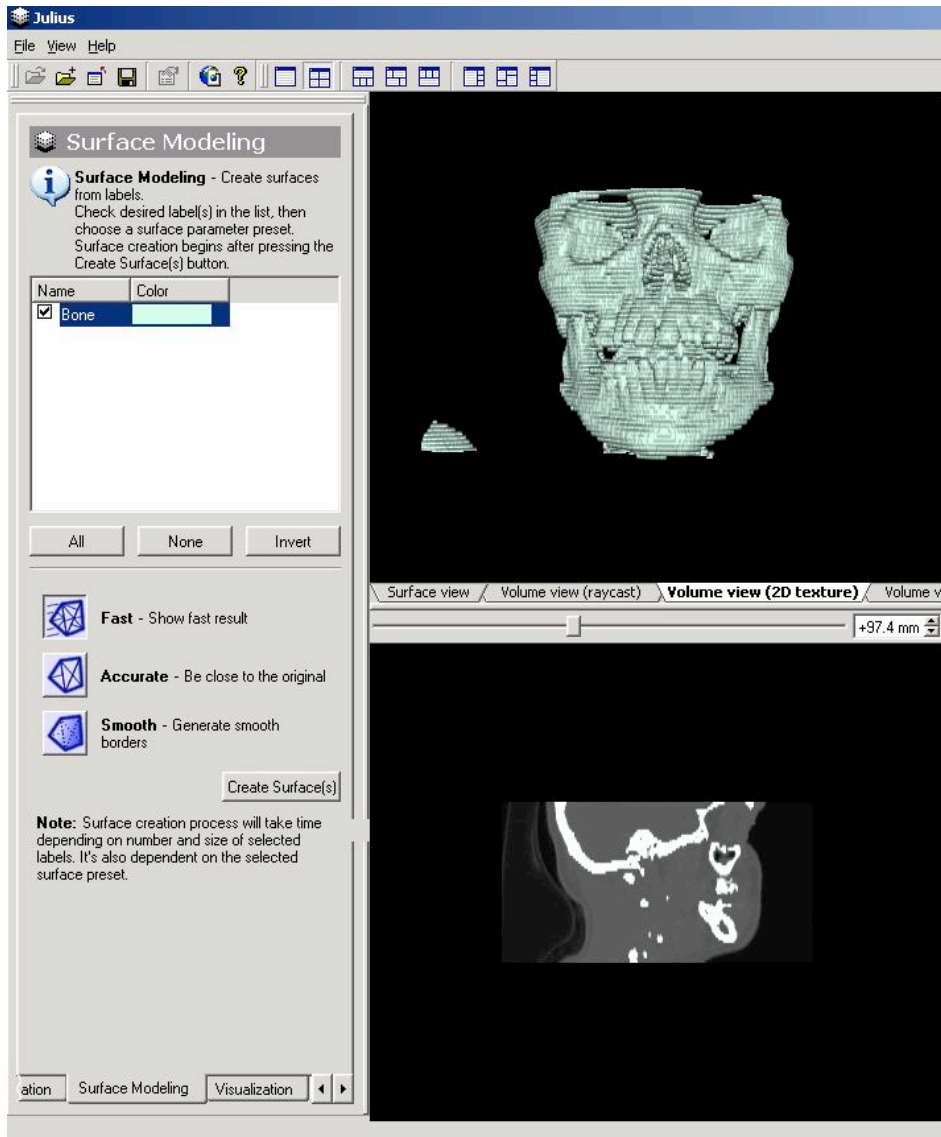
Figure 31: Screenshot of Julius showing the surface modeling interface. On the left the user can choose form the surface generation stepcard which algorithm configuration , fast, accurate or smooth, should be employed for surface reconstruction. On the right hand side bottom one can appreciate a sagittal view of the data set, whereas on the right top a 3D representation of the current segmentation is displayed

degrees. One has to consider that smoothing and reduction of triangles is a significant computational task taking up to a three or for minutes in the smoothes degree (tested on a high-end PC). For all models compared in this thesis this specific modified marching cube algorithm was used in order to make results comparable.

When using Julius the user can choose between a fast, accurate and smooth surface generation. The implementation of the marching cubes algorithm used specific for bone segmentation is chosen by accurate. The fast option is an especially efficient modification leading to quick results, whereas the smooth

option stands for more interpolation requiring more time, but producing smoother 3D surface models.

6.4 Segmentation

The 3D interactive segmentation approach was newly developed and all data sets were segmented using this technique.

This technique uses 3D texture mapping for volume rendering to visualize both the original data set and the label data set. Simplified, a given texture of high graphical detail is wrapped around a 3D structure to achieve a valuable 3D representation. In this case the structure of the skull is calculated and textured.

This well known method of volume rendering was modified so it could update the label data set in real time to give the user an initial 3D view of both data set that can be inspected from arbitrary angles and tuned in parameters for segmentation at the same time. In order to achieve this, hardware color mapping was employed. Thereby the segmentation process is directly integrated into the computational visualization pipeline and a lookup table for the color mapping is generated and scaled within two initial thresholds. Since visualization of a dynamic color mapping is hardware accelerated and can be manipulated by the user, the segmentation process is displayed in 3-D with a real-time update rate. The user can easily change upper and lower threshold values either by moving one of the two sliders or directly enter a specific value (Figure 24). This provides
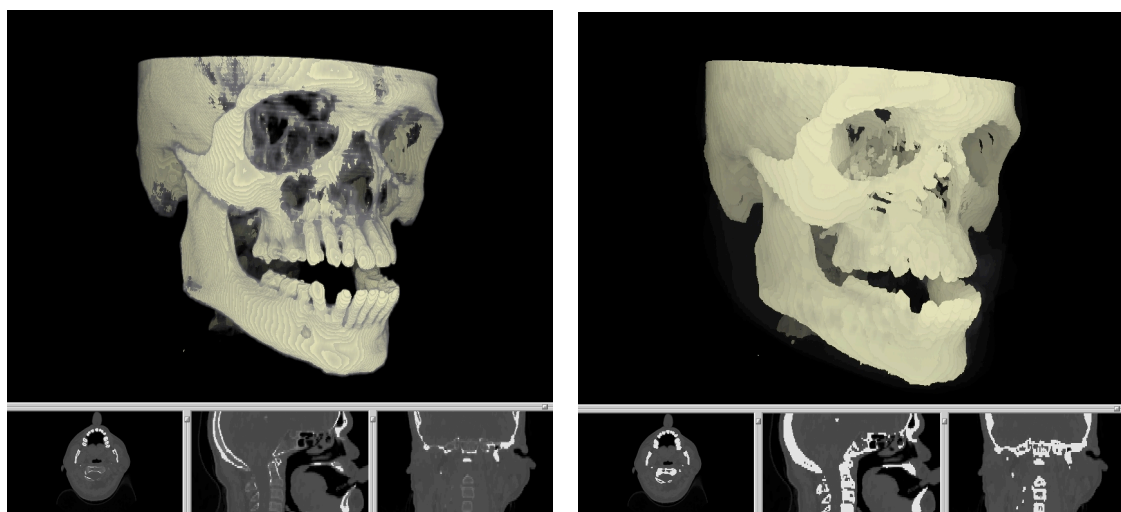

Figure 32: Segmentation Progress shown from left to right. The threshold value has been lowered and the additionally segmented bone can be appreciated in real-time.

the user with an interactive 3D view of the segmentation scene where one can appreciate the whole volume and its segmentation process in 3D at a glance. Additionally, the segmentation is visualized as an overlay on the commonly known 2-D slices of the CT scan in axial, sagittal and coronal views. Thereby delicate segmentations can still be performed.

This functionality was implemented into the software framework Julius to be able to load and easily administer the data sets and to make this tool available to the public [JUL].

Once the data was loaded the software showed an initial guess of an appropriate segmentation (See Figure 24 left). By adjusting the threshold the 3D and 2D representations were modified in real-time and a satisfying threshold to segment bone in the data set was determined (See Figure 24 right). Then the label data set was saved to disk and a 3D surface model of it was created.

6.5 Evaluation of Segmentation Algorithms

The proposed processing pipeline for CT scans was evaluated for clinical use regarding efficiency and accuracy. 3D surface models from seven cranial CT scans that were acquired for craniofacial surgical planning were generated using 3D interactive, 2D interactive threshold and manual segmentation. Prior to segmentation all dataset underwent the preprocessing pipeline outline above (i.e.
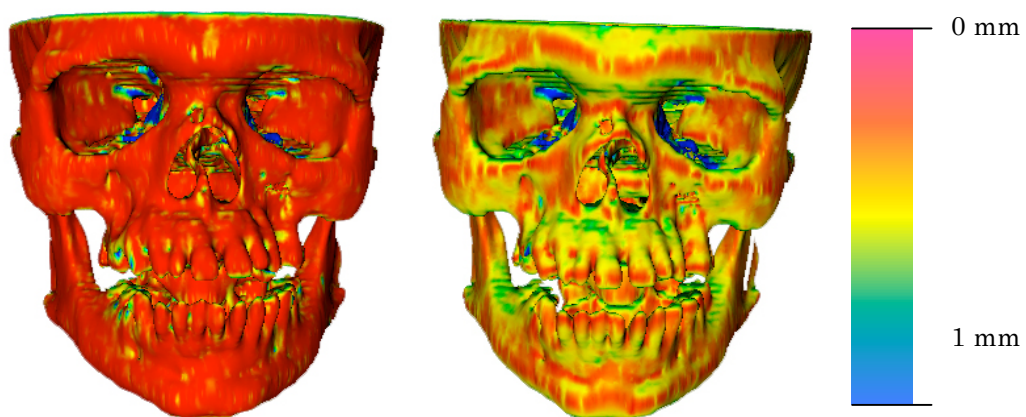

Figure 33: Surface models from manual segmentation with color-coded distances to the models derived from 3D visualized threshold on the left and 2D visualized threshold on the right. Rainbow color-code from 0 mm distance in red to 1 mm distance in blue.

Markov random field filtering, metal artifact reduction). The Hausdorff and the mean distance for each model derived from 2D and 3D visualized threshold segmentations were calculated with respect to the corresponding model from manual segmentation. To assess some parameter for efficiency we measured and

Case	3D Interactive Threshold (min)	2D Interactive Threshold (min)	Manual
1	3:11 min	3:30 min	0:55 h
2	1:20 min	3:19 min	2:12 h
3	1:14 min	1:42 min	2:18 h
4	1:38 min	2:45 min	1:30 h
5	1:42 min	2:18 min	1:50 h
6	2:10 min	2:20 min	2:15 h
7	1:41 min	2:10 min	1:45 h
Ø	**1:50 min**	**2:34 min**	**1:49 h**

Table 3: The time required to segment each of the seven cases was using 3D interactive, 2D interactive and manual segmentation was measured for one user.

compared the necessary time for 2D and 3D visualized interactive threshold segmentation.

Figure 33 exemplary visualizes the results as a color-coded distance to the reference model for one case whereas tables 3, 4 and 5 summarize distance and time measurements for all cases. These results are summarized in Figure 34.

The times for segmentation shown in table 3 were measured from a start time point to the point when the user was satisfied with the segmentation and the surface generation step could be initialized. The start point was defined to be

Case	Mean Distance Manual vs. 3D Interactive Segmentation	Mean Distance Manual vs. 2D Interactive Segmentation
1	0.351543 mm	0.405761 mm
2	0.719401 mm	0.56238 mm
3	0.487941 mm	0.52565 mm
4	0.30037 mm	0.352759 mm
5	0.360729 mm	0.634967 mm
6	0.649802 mm	0.528917 mm
7	0.79728 mm	0.586217 mm
Ø	**0.52386657 mm**	**0.51380729 mm**

Table 4: The mean distances for each model were measured comparing manual segmentation vs. 3D interactive and manual vs. 2D interactive segmentation.

when the loading process was finished and the user could actually start the segmentation.

The mean distances for all models calculated were below 1mm with an average of 0.52 mm for the mean distance between models generated from 3D segmentation and the manual reference. An average mean distance of 0.51 mm was found. The mean distances in average were essentially equal for both used methods.

The measured Hausdorff distance between the manually segmented models and the 3D interactively segmented models was found to 10.1 mm in

Case	Hausdorff Distance Manual vs. 3D Interactive Segmentation	Hausdorff Distance Manual vs. 2D Interactive Segmentation
1	8.83335 mm	9.31764 mm
2	10.0988 mm	10.9533 mm
3	9.30436 mm	9.0224 mm
4	8.79239 mm	8.65782 mm
5	9.23087 mm	9.8247 mm
6	10.8933 mm	9.70769 mm
7	14.0832 mm	8.22613 mm
Ø	**10.17661 mm**	**9.38709714 mm**

Table 5: The Hausdorff distances for each model were measured comparing manual segmentation vs. 3D interactive and manual vs. 2D interactive segmentation.
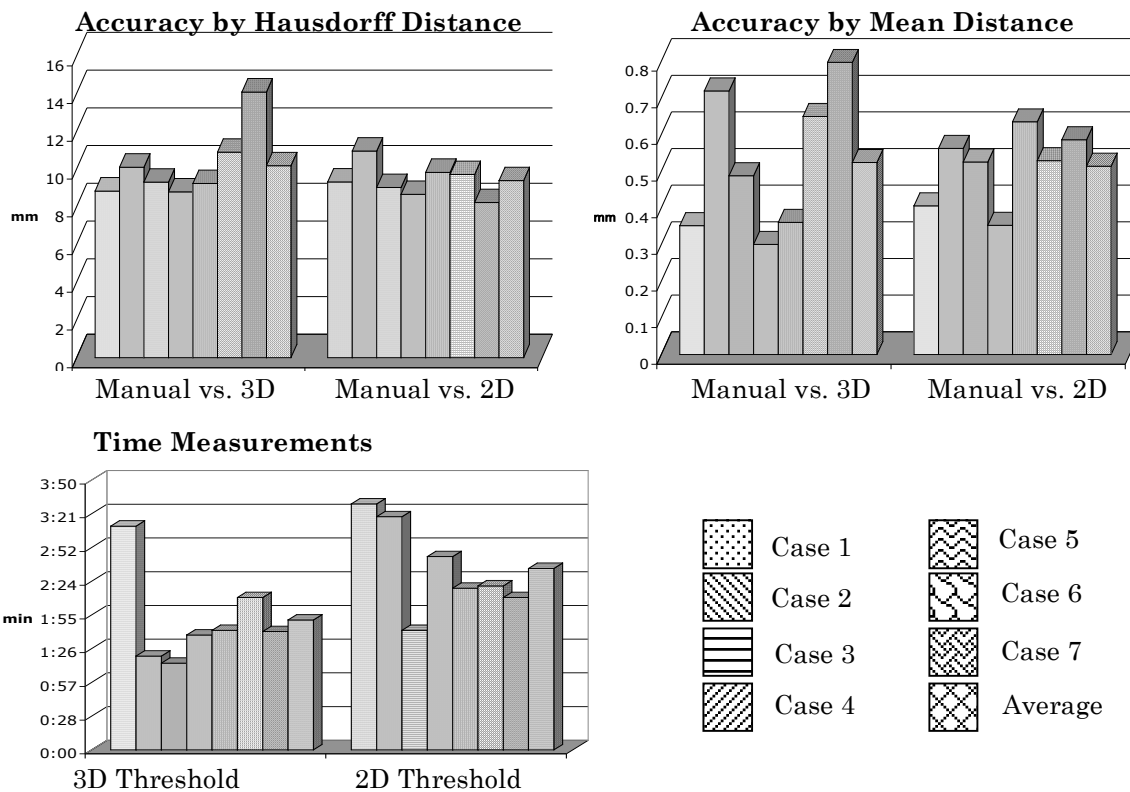

Figure 34: The top row accuracy assessments by Hausdorff and mean distance for 3D interactive and 2D interactive visualized segmentation each vs. manual segmentation is shown. On the bottom row time assessment for 3D and 2D interactive visualized segmentation is compared.

average whereas the Hausdorff distance between the manually and 2D interactively segmented models was 9.4 mm.

6.6 A Processing Pipeline For The Generation of 3D Surface Models

The previously presented results combine to pipeline of subsequent processing steps yielding a 3D surface model for computer-aided surgical planning. All processing steps were integrated into the software framework Julius offering a versatile tool for 3D surface model reconstruction from CT datasets.

Data management was one important step but is not part of the processing pipeline itself, since it can be substituted by any other way of data transfer.

For data loading the Dicom loader functionality of Julius is used. After loading the data an initial image of the dataset is shown as a 3D volume rendering and as three perpendicular 2D slice views (i.e. axial, sagittal, and coronal). Now one can either choose to filter the initial dataset by either the Markov Random field filter or the metal artifact removal filter or both. Then the user can switch to the segmentation step card within Julius and an initial label dataset with a best guess threshold value is shown as an overlay in 2D and 3D over the original dataset. Now the user can manipulate the threshold up and down by either a slider or directly enter a value. Once the user has found the optimal value the "Apply" button can be pushed and the current segmentation is saved to the label dataset. Additionally, the user can manipulate the center and width of the gray values of the CT dataset to optimize the visualization. The image is then updated on the 3D scene as well as on the 2D slice views.

Now the user can inspect the segmented dataset from all angles and slices. In case there are areas that are not satisfying yet, one can either restart the threshold segmentation, or refine the existing label dataset via manual segmentation.

Once the label dataset sufficiently represents the structure to be reconstructed to a 3D model (i.e. bone for the purpose of this thesis) one can switch to the 3D reconstruction step card within Julius and choose between the three available

surface reconstruction methods (see. Chapter 5.3.2). Then the computer calculates the 3D surface model that then can be inspected from any angle and compared to the 3D volume rendering that was initially displayed for segmentation.

7 Discussion

Results previously presented are discussed here for each step of the processing pipeline. Furthermore, the validation of the 3D interactive segmentation technique and its integration into the software framework Julius are discussed in this chapter.

7.1 Data Management

One of the most cumbersome instances in computer-aided surgery is handling different data formats. Additional problems with data handling arise when data has to be transferred outside of a clinic or private practice since certain privacy standards have to be maintained. The initial approach of mailing CD's with the data appears awkward but is certainly easy and safe. However, the introduction of a Dicom server that is able to transfer data safely over the internet is certainly much more convenient but there is a remaining risk to the privacy of patients. One solution to that is to anonymize the data prior to sending it through the Dicom server. The data management and capability of understanding different image formats is certainly very important for the success of such a pipeline and constant further development will be necessary to adapt to new upcoming format or further expansions of the Dicom format.

For this thesis all CT datasets were acquired by the same scanner, and therefore no further problems occurred ever since the first dataset was read correctly. Nevertheless, further improvement of efficiency and functionality for accessing DicomDir files is anticipated.

7.2 Image Enhancement

The Markov random fields as well as the metal artifact reduction were implemented into Julius as image post-processing steps. They served to enhance features and borders between features in the medical images in order to facilitate

the subsequent segmentation. Especially the metal artifact reduction algorithm improved the out coming models significantly.

However, the speed of the Markov random fields filter needs still to be improved. According to the statistical theory, a huge amount of calculations has to be made, slowing down the user in processing the data. As one solution to the problem, the Markov random fields filter could be automatically applied to any dataset that is loaded into Julius, saving a filtered and one unfiltered version of the data. These two versions would then be quickly available given a realistic amount of time from transferring data to actually using it. On the other hand, not using the Markov random field at all might be another solution especially when segmenting bone from CT datasets, where significant contrast can be achieved in many cases by the imaging method itself. Aside from the performance, the Markov random field method provided a standardized method to filter the data with a sophisticated algorithm yielding good results.

Regarding the metal artifact reduction algorithm it must be stated that results of the initial version used in this thesis are promising but need further evaluation and development. Especially the strong interpolating nature of the algorithm needs further adjustment. Current efforts at the surgical systems laboratory at caesar aim at improving this particular algorithm.

Finally, it can be stated that digital post-processing of any kind cannot fully compensate for major shortcomings during the scanning process. While some of these techniques can be very helpful to rule out noise and artifacts as compromising additives to the diagnostic information of radiological images, filtering algorithms must be used carefully. They change the original content of the image and can add artifacts themselves, when not properly used.

7.3 Segmentation

As the evaluation of the method shows there is an improvement of efficiency for the segmentation task. Threshold as the first algorithm implemented into this concept showed the usability of such a concept. The upcoming version of the software framework Julius has followed that concept and now all semi-automatic segmentation algorithms and manual segmentation are visualized interactively

in 3D. It is planned to integrate a whole suite of different segmentation tools that partially originate from the National Library of Medicine Insight Segmentation and Registration Toolkit (ITK). ITK is an open-source software system that employs leading-edge segmentation and registration algorithms in two, three, and more dimensions [ITK]. As one possible consequence the user is now much faster in finding the appropriate segmentation parameter and readily encounters errors that would not have been seen on a 2D view only. The new version of Julius now also supports the parallel visualization of surface models and 3D volume rendering to visually control differences between the two techniques.

Another step for improving the presented method will be to alter the current threshold technique: currently only straight values are applied as opposed to new techniques that statistically analyze the given gray value distribution and suggest a certain threshold distribution for specific structures (i.e. cortical bone, bone marrow, teeth etc). Together with the concept of anatomical nomenclature leading the segmentation one can envision a system that suggest a certain threshold upon pressing one of the listed anatomical structures. This structure is then visualized in 3D leaving the user the option to manipulate the given threshold. This manipulation would be registered and saved in a data bank along with the specifics of the CT data set. Thereby the first guess threshold by this system would improve over time with more segmentation done. Finally, an almost perfect guess for the first threshold could be achieved.

Another improvement of threshold segmentation would be to apply different threshold values to a particular region of the data set. For example one problem that could be addressed is to segment teeth better: teeth are denser than bone and therefore one could apply a different threshold to the region of teeth.

However, the traditional perpendicular slice views are still required and helpful to verify segmentations in a view that most medical professionals are used to. Especially manual segmentation can be expected to remain a domain of a slice-by-slice approach. But now the varied segmentation in 2D can be directly visualized in 3D parallel to the 2D slice views. This again offers the advantage of not having to generate a surface model.

7.4 Evaluation of 3D Interactive Segmentation

Despite the availability of software for surgical planning the validation of the used algorithms for segmentation is a complex, still unsolved scientifically challenging problem. While the segmentation of mathematical and physical models has an easily accessible ground truth for verification, results are not fully applicable to the complexity of real human anatomy. On the other hand the ground truth evaluation of real patient data is difficult not because there is no ground truth, but it cannot be accessed in a way that can be easily used [Kap96]. Several methods for validation have been described. Visual inspection by medical experts is the most straightforward approach while obviously being subjective [Bru93]. The statistical comparison to manual segmentations done by experts seems to be less subjective but time consuming. Moreover manual segmentations vary between observers depending on the complexity of a structure for about 15% [Kik92]. Another possibility is to validate segmentations based on fiducial markers placed in specific structures of cadavers. These can be reencountered on the radiological images as well as in real life [Gob94]. While this approach seems capable to provide accurate results it appears very cost and labor intensive.

Current research at the National Institute of Health aims at providing a public available validation suite escorted by validation data sets. The essential design elements include truth generation, the concept of blind evaluation or scoring, the use of multiple observers to capture the variation in the human decision process, and the analysis of the output through statistical analysis [Yoo00]. Since this initiative has just recently started there are no tools available to the public, yet. However, some of the principles, as truth generation and statistical analysis of the output were adapted to this study.

The small number of cases and the fact that only one observer segmented them do not justify a statistical conclusion from this study. It can be rather seen as a proof of principle. Nevertheless, the assessment indicates that volume visualization has a positive effect on time efficiency even for such simple segmentation algorithms as threshold.

Three additional aspects should be considered when interpreting these results. First, manual segmentation was performed as initial 2D threshold and further manual refinement. Therefore a major part of the 3D model defined as standard from manual segmentation derives from 2D visualized threshold and is therefore biased by this method. This could partially explain the smaller distances found between manual and 2D threshold in this study.

As a second aspect, the segmentation times for 2D interactive segmentation were measured without any surface generation. Even though it can be stated that the 3D interactive visualized threshold achieves approximately the same accuracy as 2D interactive segmentation but in shorter time. However, intermittent surface generation can be frequently observed when segmentations for clinically applied 3D models is performed. Therefore the improvement of time efficiency is probably underestimated in our assessment. This certainly underestimates the efficiency of the proposed method, but there was no data found in the literature showing how many surfaced generations are approximately performed for a segmentation of a skull. Neither was it possible to assess this number in scientific way, nor would it seem reasonable to guess an amount of time and simply add this extra time to the time needed for 2D threshold segmentation.

The third aspect concerns the 3D model generation. Using the same modified marching cube algorithm to reconstruct the 3D surface model makes it difficult to compare the 3D models because this special modification could only be applied to threshold segmentations. This is inherently the only segmentation this modification benefits from since it takes those threshold values into account. However, a 3D surface model from manual segmentation was taken as reference where this particular functionality of the algorithm cannot be used.

As an indicator for the usability of 3D interactive applications in computer-aided surgery one may consider the increasing number of software packages, especially in the commercial sector, that take advantage of volume rendering. It can be expected that with increasing hardware capabilities of future computer generations volume rendering may fully replace the currently used 3D surface models for computer-aided surgical planning. As a step between the work described in thesis might be seen.

7.5 3D Model Reconstruction

The adjusted marching cube algorithm for surface reconstruction showed good results when used for threshold segmentation. The close relationship to the threshold technique yielding gray values instead of a strictly binary label map made it easy to apply this method for gray value based surface reconstruction. However, for most other segmentation techniques the limitation of a binary label map has to be overcome. Extrapolation from the label map back to the original gray values could be one solution to that problem, which is now further investigated at the surgical systems laboratory at caesar.

Besides the marching cube algorithm there exist a number of other surface generation methods that were not investigated in this study. Potentially some of them are more suitable for reconstruction of bone as needed in this thesis, even though there are no such reports in the literature. However, there are many other modifications of the marching cube itself reported in the literature, that aim at improving performance by either reducing the number of triangles created [Lee01] or more efficient calculation [Del01].

Increasing computer hardware power can be expected to sooner or later provide the power to replace surface models fully by volume rendering since surface rendering inherits some disadvantages so far accepted for performances reasons:

Surface rendering is restricted to display segmented data sets. These can be affected by false segmentation or iso-surface values. Moreover, most reconstruction algorithms contain some kind of interpolation altering the original image content. If a surface construction proves to be affected by errors or artifacts the whole reconstruction process has to be redone usually taking several minutes.

Nevertheless, given technical capabilities at this moment, 3D surface models offer the unique opportunity to interact with the surface models as for example to cut parts and move them arbitrarily in the 3D scene. This is the basis for interactive surgical simulations or virtual surgical planning.

7.6 *Julius – a General Software Framework*

The software framework Julius offered the basic functionality to implement the idea of 3D interactive segmentation showing its biggest advantage compared to other software packages: it can be easily expanded and new functionality can be readily added. It is the clearly structured modular concept of Julius not restricting developers that makes such quick implementations possible. Furthermore the two filtering algorithm as well as the dedicated implementation of the marching cubes algorithm were integrated into the software framework.

Since the development of Julius has started in 1999 not quite as much functionality is available as there it for other software packages. For example Analyze exceeds Julius by far in terms of different functions and tools. On the other hand software packages that have been developed for a long time do not apply the latest implementation and software development techniques. Two possible consequences are the deceleration of the further development and cumbersome user interfaces. To overcome this limitations and expand the range of available image enhancement and segmentation algorithms current efforts of the Julius developers aims at integrating a whole library for image segmentation and enhancement algorithms. This library is provided and developed freely by the National Library of Medicine, U.S.A. [ITK].

8 Conclusion

A comprehensive processing pipeline for generating 3D models for computer-aided applications in craniofacial surgery has been developed and evaluated. This pipeline consists of two filtering steps, a 3D interactive segmentation algorithm and a dedicated implementation of the marching cubes surface reconstruction algorithm. All processing steps were integrated into the software framework Julius combining to a versatile tool for generating 3D models. The integrated pipeline was tested for seven different CT datasets of varying craniofacial pathologies. 3D visualized threshold segmentation compared to 2D visualized threshold segmentation regarding efficiency and accuracy showed. Accuracy differences between the two methods whereas the 3D visualized method showed an improvement in efficiency.

For filtering a Markov random fields based and a metal-artifact removal algorithm were applied. A 3D interactive visualized segmentation based on a threshold technique was developed and compared to 2D visualized threshold segmentation as well as manual segmentation. Criteria tested for were efficiency in terms of required user interaction time and accuracy whereas manual segmentation was taken as reference. A marching cube algorithm taking user defined threshold parameters directly into account achieved surface reconstruction. This method is capable of preserving details in bony structures. Data was successfully managed and transferred by the commercial Dicom server Pmod [PMO].

For the future it is planned to refine and speed up the concept of 3D interactive visualization. The current version of Julius provides 3D interactive visualization for all manipulations that are taking place on the dataset. Certainly the response time and handling have to be improved further. With acceleration of computer hardware it can be expected that in the future most segmentation algorithms will be visualized in 3D interactively. However, it will take the hearts and minds of the surgeons to accept other than the well known slice view and for some instances the slice view will certainly remain the most advantageous view.

9 Acknowledgements

10 References

[Ada94] Adams R., Bischof L., *"Seeded based region growing,"* IEEE Trans. Pattern Recogn. Mach. Intell., Vol 16 No. 6, (1994) pp 641-647

[AMI] *amira.zib.de*

[ANA] *www.mayo.edu/bir/home.html*

[Bal00] Baldock R., Graham J., *"Image Processing and Analysis – a practical approach,"* Oxford University Press, Oxford, 2000.

[Ban00] Bankman I.N., *"Handbook of medical imaging – Processing and Analysis,"* Academic Press, 2000

[Bat90] Batnitzky S, Rosenthal SJ, Siegel E, Wetzel LH., Murphey MD, Cox GG, McMillan JH, Templeton AW and Dwyer SJ 3d., *"Teleradiology: an assessment,"* Radiology, Vol. 177, (1990) pp. 11-17

[Ber86] Bernsen J., *"Dynamic threshold of gray-level images."* Proc. 8th Int. Conf. Pattern Recognition, Paris, France, (1986) pp. 1251-55

[Bid92] Bidgood, D., Horii, S. C., *"Introduction to the ACR-NEMA DICOM standard,"* Radiographics, Vol. 12(2), (1992) pp. 345- 355

[Boy83] Boyd D. P., Lipton M. J., *"Cardiac computed tomography,"*
Proc. IEEE, Vol. 71, (1983) pp. 298-307

[Bru93] Brummer, M., Mersereau, R., Eisner, R., Lewine, R., *"Automatic detection of brain contours in MRI data sets,"* IEEE Transactions on Medical Imaging, Vol. 12(2), (1993) pp. 153-166

[Car94] Cardoza J.D., Herfkens R.J., *"MRI Survival Guide,"* Raven Press Ltd., New York, 1994.

[Csi99] Csillag A*., "Anatomy of the Living Human – Atlas of medical imaging,"* Könemann Verlagsgesellschaft, Köln, 1999.

[Doe00] Doessel O., *"Bildgebende Verfahren in der Medizin,"* Springer Verlag, Berlin, 1999.

[Del94] Delingette, H., Subsol G., Cotin S., Pignon J.. *"A craniofacial surgery simulation testbed,"* Research report RR-2199, INRIA, 1994.

[Del01] Delibasis KS, Matsopoulos GK, Mouravliansky NA, Nikita KS. *"A novel and efficient implementation of the marching cubes algorithm,"* Comput Med Imaging Graph., ;Vol. 25(4), (2001) pp.343-52

[Ehr97] Ehricke, H.-H., *"Medical Imaging – Digital Bildanalyse und – kommunikation,"* Vieweg Verlag, 1997.

[Eng99] Engelmann U.*, "Borderless Teleradiology with CHILI,"* J Med Internet Res. Vol. 1(2),e8, 1999

[Eve00] Everett P., Seldin EB., Troulis M., Kaban LB., Kikinis R. *"A 3D System for Planning and Simulating Minimally-Invasive Distraction Osteogenesis of the Facial Skeleton,"* Proceedings of Third International Conference On Medical Robotics, Imaging and Computer Assisted Surgery, (2000) pp. 1029-1039

[Fer00] Ferrant M., Warfield S., Nabavi A., Jolesz F.A., Kikinis R., *"Registration of 3D Intraoperative MR Images of the Brain Using a Finite Element Biomechanical Model,"* Proceedings of Third International Conference On Medical Robotics, Imaging and Computer Assisted Surgery, (2000) pp.19-28

[Gem84] Geman, S. Geman, D. *"Stochastic relaxation, Gibbs distributions and the Bayesian restoration of images,"* IEEE Transactions on Pattern Analysis and Machine Intelligence, Vol. 6, (1984) pp. 721-742

[Ger99] Gering D., Nabavi A., Kikinis R., Grimson W. E. L., Hata N., Everett P., Jolesz F., Wells III W., *"An Integrated Visualization System for Surgical Planning and Guidance using Image Fusion and Interventional Imaging,"* Proceeding of Medical Image Computing and Computer-Assisted Intervention (MICCAI), Cambridge England, (1999) pp.809-819

[Ger01] Gerig G., Jomier M., Chakos M.*, "Valmet: A new validation Tool for Assessing and Improving 3D Object Segmentation,"* Fourth International Conference on Medical Image Computing and Computer-Assisted Intervention MICCAI 2001, pp. 516-523

[Gob94] Gobel, J., Snell, J., Hinckley, K., Kassell, N., *"A real-time system for 3D neurosurgical planning,"* Proceedings of the Third Conference on Visualization in Biomedical Computing. SPIE Proceeding Vol. 2359, (1994) pp. 552-563

[Gol95] Goldman L.W., Fowlkes J.B., *"Medical CT and Ultrasound – Current Technology and Applications,"* Proceedings of the 1995 Summer School on CT and US Technology and Applications of the American Association of Physicists in Medicine, 1995

[Grei90] Greinacher CFC, Bach EF, Herforth M, Luetke B, Senfert G. *"Computer-assisted radiology - requirements and solutions for digital diagnostic imaging,"* Medical Informatics, Vol. 15(1), (1990) pp. 21-29

[Has97] Hassfeld S., Raczkowsky J., Bohner P., Hofele C., Holler C., Mühling J., Rembold U., *"Robotics in oral and maxillofacial surgery. Possibilities, chances, risks,"* Mund Kiefer Gesichtschir, Vol. 1, (1997) pp. 316-323

[Has98] Hassfeld S., Mühling J., *"Navigation in maxillofacial and craniofacial surgery,"* Comp Aid Surg, Vol. 3, (1998) pp. 183-187

[Hel98] Held K., Rota Kopps E., Krause B., Wells W., Kikinis Muller-Gartner R., H., *"Markov Random Field Segmentation of Brain MR Images,"* IEEE Transactions on Medical Imaging, Vol.16, (1998) pp. 878-887

[Hoh92] Höhne K.-H., Hanson W.A., *"Interactive 3D-segmentation of MRI and CT volumes using morphological operations,"*. J. Comput. Assist. Tomogr. Vol 16, 2, (1992) pp. 285-294

[Hor96] Hornak J.P., *"The Basics of MRI,"* www.cis.rit.edu/htbooks/mri/inside.htm, 1996.

[Hou73] Hounsfield G. N., *"Computerized transverse axial scanning (tomography). Part 1: Description of system,"* Br J of Radiol, Vol 46, (1973) pp. 1016-22

[IMJ] *rsb.info.nih.gov/ij/*

[ITK] *www.itk.org*

[JPG] Pennebaker W., Mitchell J., *"JPEG - Still image data compression standard,"* Van Nostran Reinhold, New York, 1993.

[JUL] *www.julius.caesar.de*

[Kal87] Kalender W. A., Hebele R., Ebersberger J., *"Reduction of CT artifacts caused by metallic implants,"* Radiology Vol. 164(2), (1987) pp. 576–577

[Kap96] Kapur T., Grimson W. E. L., Wells W.M., Kikinis R., *"Segmentation of Brain Tissue from Magnetic Resonance Images,"* Medical Image Analysis, Vol. 1(2) 1996

[Kee97] Keeve E., Schaller S., Girod S., Girod B., *"Adaptive Surface Data Compression,"* Signal Processing, Vol. 59, No. 2, (1997) pp. 211-220

[Kee98] Keeve E., Girod S., Kikinis R., Girod B., *"Deformable Modeling of Facial Tissue for Craniofacial Surgery Simulation,"* Computer Aided Surgery, John Wiley & Sons Inc., New York, invited paper, Vol. 3, No. 5, (1999) pp. 228-238

[Kik92] Kikinis, R., Shenton, M., Jolesz, F., Gerig, G., Martin, J., Anderson, M., Metcalf, D., Guttmann, C., McCarley, R., Lorensen, W., and Cline, H.,

"Quantitative Analysis of Brain and Cerebrospinal Fluid Spaces with MR Imaging," JMRI, Vol. 2, (1992) pp. 619-629

[Kro00] Krol Z., *"Registration of Intra-Modal Medical Images Using a Novel S-Distance Approach,"* Proceedings Bildverarbeitung für die Medizin 2000, Munich, March 12-14, 2000

[Kro01] Krol Z., Zerfass P., Rymon-Lipinski B., Jansen T., Zeilhofer H.-F., Sader R., Keeve E.*, "Computer Aided Osteotomy Design for Harvesting Autologous Bone Grafts in Reconstructive Surgery,"* Proceedings SPIE Medical Imaging MI'01, San Diego, CA, February 17-23, 2001.

[Kru01] Krupinski E., Radvany M., Levy A., Ballenger D., Tucker J., Chacko A., VanMetter R., *"Enhanced visualization processing: effect on workflow,"*
Acad Radiol.,Vol. 8(11), (2001) pp. 1127-1133

[Kum75] Kumar A., Welti D., Ernst R.R., *"NMR Fourier Zeugmatography,"*
J Magn Reson, Vol. 18, (1975) pp. 69-83

[Lee01] Lee T. Y., Lin C.H., *"Growing-cube isosurface extraction algorithm for medical volume data,"* Comput Med Imaging Graph., Vol. 25(5), (2001) pp. 405-15

[Lie01] Lievin M., Hanssen N., Zerfass P., Keeve E., *"3D Markov Random Fields and Region Growing for Interactive Segmentation of MR Data,"* Fourth International Conference on Medical Image Computing and Computer-Assisted Intervention MICCAI'01, Utrecht, October 14-17, 2001

[Lor87] Lorensen W. E., Cline H. E.*, "Marching Cube: A High Resolution 3D Surface Construction Algorithm,"* Computer Graphics, Vol. 21, No. 4, (1987) pp. 163-169

[Mai98] Maintz J. B. A., Viergever M. A., "*A survey of medical image registration,*" Med. Image Anal., Vol. 2 (1), (1998) pp. 1--36

[Mar98] Marmulla R., Niederdellmann H., *"Computer-aided navigation in secondary reconstrucion of post-traumatic deformities of the zygoma,"*
J Craniomaxillofac Surg, Vol. 26, (1998) pp. 68-69

[MIM] *www.materialise.com*

[Pal93] Pal N.R., Pal S.K.*, "A review on image segmentation techniques,"* Pattern Recognition, Vol 26, No. 9, (1993) pp. 534-544

[Pfl01] Pflesser B., Petersik A., Pommert A., Riemer M., Schubert R., Tiede U., Höhne K-H., *"Exploring the Visible Human's Inner Organs with the VOXEL-MAN 3D Navigator,"* In James D. Westwood, H.M. Hoffman, G.T. Mogel and D.

Stredney (eds.): Medicine meets Virtual Reality, Proc. MMVR 2001, Health Technology and Informatics Vol. 81, IOS Press, Amsterdam, (2001) pp. 379-385

[Obr01] O'Brien D.F., Roberts G.A., Pidgeon C.N.*,"Quality evaluation of spiral CT-directed skull base coordinate assignment using the Leibinger 'Z-D' frame and 'STP' software,"* Br J Neurosurg Vol 15(6), (2001) pp. 479-84

[Odl01] Odlum O., *"A method of eliminating streak artifacts from metallic dental restorations in CTs of head and neck cancer patients,"* Spec Care Dentist, Vol. 21(2), (2001) pp. 72-4

[OSI] *www.expasy.org/www/UIN/html1/projects/osiris /osiris.html*

[Pel96] Pelizzari SA, Grzeszczuk R, Chen GT, Heimann R, Haraf DJ, Vijayakumar S, Ryan MJ *"Volumetric visualization of anatomy for treatment planning,"* Int J Radiat Oncol Biol Phys., Vol. 34(1), (1996) pp. 205-11

[PMO] *www.pmod.com*

[QT] *www.trolltech.com*

[Ric98] Richolt J., Golland P., Winalski C. S., Anderson M., Bhalero A., Koskinen S., Martin S., Kikinis, R. *"The Digital Interactive Knee Atlas,"* American Academy of Orthopedic Surgeons Annual Meeting, Multimedia Education Demonstrations, New Orleans, LA, March 1998.

[Rus99] Russ C., *"The Image Processing Handbook,"* CRC Press, Boca Raton,1999

[Sai98] Saiviroonporn P., Robatino A., Zahajszky J., Kikinis R., Jolesz F.A., *"Real Time Interactive 3D-Segmentation,"* Acad. Radiol. Vol. 5, (1998) pp. 49-56

[Sch99] Schramm A., Gellrich B.C., Gutwald R., Thoma L., Schmelzeisen R., *"Reconstructive computer assisted surgery of deformities by mirroring CT data sets,"* Med Biol Eng Comp, Vol. 37, (1999) pp. 644-645

[Sha99] Shareef N., Wand D.L., Yagel R., *"Segmentation of medical images using LEGION,"* IEEE Trans. Med. Imag., Vol. 18 No. 1, (1999) pp. 74-91

[SLI] *www.Slicer.org*

[SPL] *www.spl.harvard.edu:8000*

[Tay96] Taylor R. H., Lavallee S., Burdea G. C., Mösges R., *"Computer-Intergrated Surgery,"* MIT Press, Cambridge 1996

[TCL] *www.tcl-tk.net*

[TDK] *www.tdk.com/tdkmedical/HTML*

[Wan99] Wang G., Vannier M.W., *"Computerized tomography,"* Encyclopedia of Electrical and Electronics Engineering, edited by Webster JG, John Wiley & Sons, New York, 1999.

[Van83] Vannier M.W., Marsh J.F., Warren J.O., *"Three-dimensional computer graphics for craniofacial surgical planning and evaluation,"* Computer Graphics, Vol. 17(3), (1983) pp. 263--273

[VTK] *www.kitware.com/vtk.html*

[Wes97] Westin C-F., Bhalerao A., Knutsson H., Kikinis R., *"Using Local 3D Structure for Segmentation of Bone from Computer Tomography Images,"* IEEE Conference on Computer Vision and Pattern Recognition (1997), San Juan, Puerto Rico

[Wes98] Westin C.F., Warfield S., Bhalerao A., Mui L., Richolt L., Kikinis R., *"Tensor Controlled Local Structure Enhancement of CT Images for Bone Segmentation,"* Proceedings MICCAI'98, Lecture Notes in Computer Science, LNCS, Vol 1496, (1998) pp. 1205-1212

[Woo01] Woodward, P., *"MRI for Technologists,"* McGraw-Hill, New York, 2001

[Yoo00] Yoo T. S., Ackerman M. J., Vannier M., *"Toward a Common Validation Methodology for Segmentation and Registration Algorithms,"* Third International Conference on Medical Image Computing and Computer-Assisted Intervention, MICCAI'00, Vol. 1935, (2000) pp. 422-431

[XME] *xmedcon.sourceforge.net/*

[XML] *www.w3.org/XML/*

[Zei94] Zeilhofer H-F., Sader R., Horch H-H., Wunderlich AP., Kirsten R., Gerhardt HCP*.," Computer-assisted individual osteotomy design for mandibular recostruction,"* Visual Data Exploration and Analysis, San Jose, Proceedings SPIE. Vol 2178, (1994) pp. 197-205

[Zeil97] Zeilhofer H.-F., Krol Z, Sader R., Hoffmann K.-H., Hogg M., Schwaiger P., Horch H.-H., *"Multidimensional Images in Diagnostics of Head and Neck Area Using Efficient Registration and Visualization Methods,"* Proceedings Computer Assisted Radiology CAR'97, Berlin, Germany, (1997) pp. 723-728

[Zeil99] Zeilhofer H-F, Sader R, Apostoloscu V, Hoffmann K-H, Poth U, Kliegis U.,*"Cybernavigation in Cranio-Maxillofacial Surgery,"* Proceedings TERENA NordUnetNetworking Conference „The challenge of gigabit networking", Lund,1999

11 Figures and Tables

11.1 Figures

11.2Tables